cells in 10 crypts of the normal mucosa and in the mucosa-bordering ulcers (5 mm from the ulcer edges).

### Measurement of TNFα and Interferon γ in Colon Tissues

Colon tissues were homogenized in cold PBS and centrifuged at 20,000*g* for 15 minutes at 4 °C. We determined the total protein in the supernatants with a Protein Assay Kit (Bio-Rad, Hercules, Calif.), and TNFα and interferon γ (IFNγ) levels were measured with an enzyme-linked immunosorbent assay (ELISA) kit (DIACLONE SAS, Besancon, France) according to the manufacturer's instructions.

### Statistical Analysis

Unless otherwise specified, data are expressed as mean ± SD. Statistical parameters were ascertained with Statview J-4.5 software (Abacus Concept, Berkeley, Calif.). The differences between means were compared by the unpaired Student *t* test. Values of $P < 0.05$ were considered significant.

## RESULTS

### Administration of Recombinant Human HGF Reduced DAI Scores in Rats with Large Colonic Ulcers Induced by TNBS

To evaluate the degree of TNBS-induced colitis before HGF administration, we performed colonoscopic examinations on day 5. Although rectal administration of TNBS induced ulcers in the large intestines of all rats, approximately 80% of the animals exhibited large ulcers occupying more than two thirds of the luminal circumference (Fig. 1A). Only rats suffering from these larger colonic ulcers underwent treatment with intravenous recombinant human HGF.

We evaluated body weight changes and DAI scores of TNBS-induced colitis rats treated with PBS or HGF (Fig. 2). Body weights decreased until 5 days after TNBS administration and then gradually increased. Treatment with HGF did not affect sequential changes in body weight (Fig. 2A). However, in TNBS colitis rats given human HGF, the DAI scores were significantly reduced (3.7 ± 0.7) compared with those given only PBS (5.1 ± 0.4) by day 10 ($P = 0.0001$; Fig. 2B).

### HGF Administration Facilitated the Repair of Colonic Ulcers and Reduced Colitis-induced Shortening of the Large Intestine

Because experimental colitis induced by a single enema of 7.5 mg TNBS spontaneously disappeared within 12 to 14 days, the colonic ulcers and the lengths of the large intestine were examined in rats treated with either PBS or HGF on day 10. Before death, we evaluated colonoscopic appearance in PBS- or HGF-treated rats (Fig. 1B). In PBS-treated rats, the depth of colonic ulcers was slightly reduced compared with

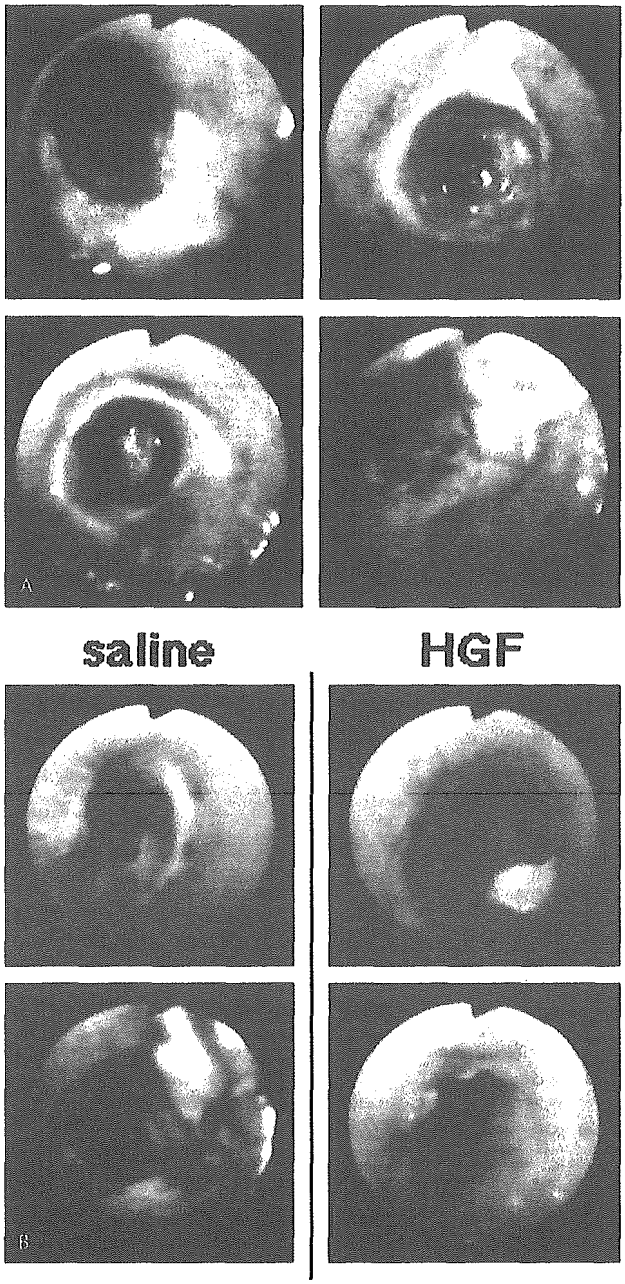


**FIGURE 1.** Representative colonoscopic appearances of large colonic ulcers in TNBS-administered rats. A, colonoscopies were performed 5 days after a single enema of TNBS (7.5 mg/rectum). Administration of TNBS induced large and deep colonic ulcers that occupied more than two thirds of the luminal circumference in 80% of rats. B, on day 10, rats treated with PBS or recombinant human HGF were subjected to colonoscopies. Rats treated with PBS exhibited large colonic ulcers that bled readily from the bordering mucosa, whereas those treated with HGF exhibited reduced ulcer size and mild contraction of the mucosa surrounding healing ulcers.

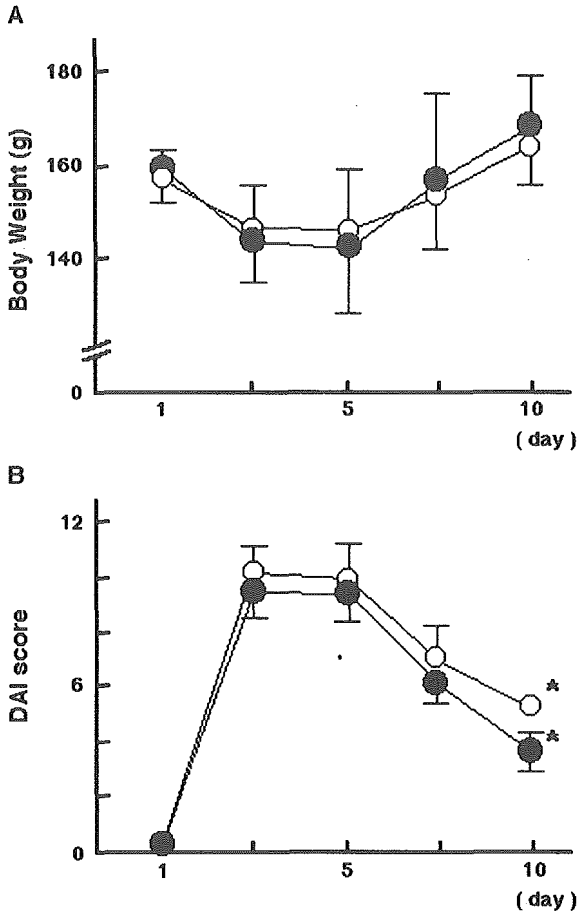


FIGURE 2. Intravenous HGF administration reduces disease activity but does not affect changes in body weight in rats with TNBS-induced colitis. After rectal TNBS administration, sequential changes in body weight (A) and DAI (B) were examined in PBS- or HGF-treated rats (○, n = 8; ●, n = 9). Although the intravenous injections of recombinant human HGF for 5 days did not affect the changes in body weight, the disease activity in rats treated with HGF was significantly reduced on day 10 (*, $P = 0.0001$).

those developed by day 5 after a single enema of TNBS (Fig. 1A), but the large colonic ulcers still remained, and bleeding from the bordering mucosa occurred readily. In contrast, HGF-treated rats exhibited remarkable amelioration of colonic ulcers, with mild contraction of the surrounding mucosa (Fig. 1B). After death, we measured the areas of colonic ulcers and the colon lengths (Fig. 3). In TNBS-induced colitis rats treated with recombinant human HGF, the areas covered by ulcers within the large intestine were significantly reduced in size (54.4 ± 32.3 $mm^2$) compared with those treated with PBS (112.8 ± 61.2 $mm^2$; $P = 0.037$; Fig. 3A), and the colons were significantly longer (13.3 ± 0.7 cm) than those in PBS-treated rats (11.8 ± 1.7 cm; $P = 0.043$; Fig. 3B).

## Intravenous Injection of Human HGF Enhances the Regeneration of the Colonic Epithelium and Decreases the Inflammatory Cell Infiltrate in Rats with TNBS Colitis

We also evaluated the effect of HGF on TNBS-induced colonic ulcers in rats by histologic analysis. In TNBS-induced colitis rats treated with PBS, extensive mucosal damage, inflammatory cell infiltrates, and edema were observed on day 10 (Fig. 4A). After treatment with recombinant human HGF for 5 days, rats with TNBS colitis had an enhanced regenerative epithelium and a decrease in inflammatory cell infiltrates (Fig. 4A). Consequently, HGF administration significantly reduced the histologic score to 4.3 ± 0.9 compared with 5.4 ± 0.9 for PBS-treated rats ($P = 0.030$; Fig. 4B). Next, we measured MPO activity in normal or TNBS-inflamed colon tissues with or without HGF treatment to evaluate the degree of inflammation. Although the MPO activity was significantly increased in TNBS-inflamed colon tissues (12.29 ± 0.98 U/g wet tissue on day 10 compared with 0.75 ± 0.44 for normal colon tissues; $P = 0.0009$), administration of recombinant human HGF significantly reduced the accumulation of MPO in TNBS-inflamed colons by approximately 50% (6.41 ± 1.94 U/g wet tissue; $P = 0.0013$).

We examined the BrdU labeling index to evaluate the proliferation of the colonic epithelium (Fig. 5). In TNBS colitis rats treated with PBS, BrdU-positive epithelial cells at the edges of ulcers increased to 12.2 ± 7.9/crypt compared with those in normal mucosa (1.7 ± 2.1/crypt). When the rats were treated with recombinant human HGF, we observed a significant increase in BrdU-positive cells within both the mucosal epithelium surrounding colonic ulcers (30.4 ± 2.4/crypt) and the normal mucosal epithelium (11.3 ± 1.5/crypt; $P = 0.047$ and 0.004 in comparison with PBS-treated rats, respectively; Figs. 5, A and B).

## TNBS-induced Colitis Rats Treated with Recombinant Human HGF Exhibited Reductions in TNFα and IFNγ in Colon Tissues

Because rats treated with human HGF exhibited a reduction in inflammatory cell infiltrates, we examined colonic tissue levels of TNFα and IFNγ (Fig. 6). After administration of TNBS, tissue levels of TNFα were 20.8 ± 3.5 and 20.2 ± 2.9 (pg/mg protein) on days 5 and 10, respectively (Fig. 6A). Colonic TNFα levels were 13.6 ± 4.8 pg/mg protein on day 10 in rats treated with recombinant human HGF ($P = 0.028$). Levels of IFNγ in colon tissues on day 5 (23.8 ± 3.9 pg/mg) were similar to those in normal rats (day 0; 19.5 ± 10.0 pg/mg; Fig. 6B). TNBS-induced colitis rats given PBS exhibited a significant increase in colon tissue IFNγ on day 10 (51.1 ± 13.7 pg/mg) compared with those on day 5 ($P = 0.003$). In rats treated with recombinant human HGF, the IFNγ level in colon

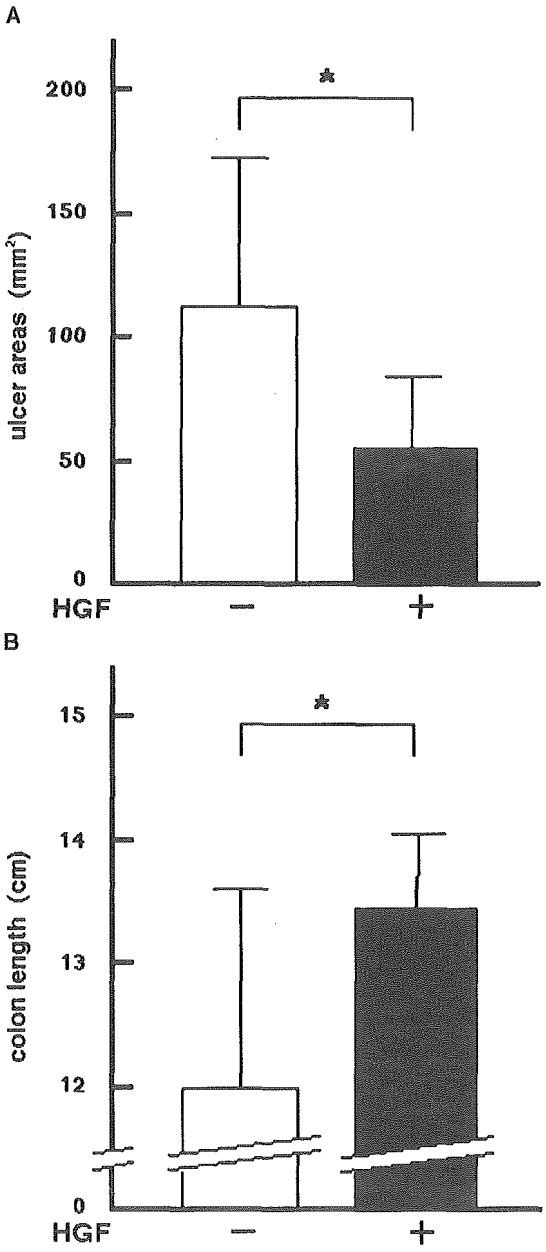


**FIGURE 3.** Administration of HGF reduces colonic ulcers and prevents shortening of the large intestine in rats with TNBS-induced colitis. The areas of the colonic ulcers and the lengths of the large intestines in PBS- or HGF-treated rats with TNBS-induced colitis (n = 8 or 9, respectively) were determined on day 10. A, the areas of colonic ulcers in rats treated with recombinant human HGF were significantly reduced compared with ulcers in PBS-treated rats (*, $P = 0.037$). B, the large intestines of rats treated with HGF were significantly longer than those treated with PBS (*, $P = 0.043$).

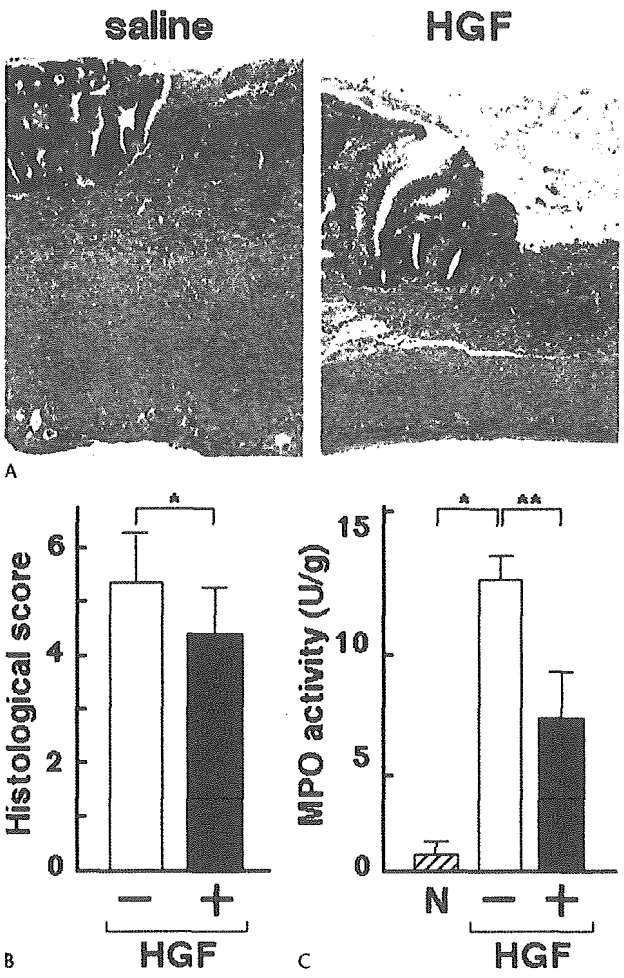


**FIGURE 4.** Intravenous injection of recombinant HGF enhances colonic epithelium regeneration and decreases the inflammatory infiltrate in rats with TNBS-induced colitis. Large intestines, which were obtained on day 10 from colitis rats treated with PBS or HGF (n = 8 or 9, respectively), were opened longitudinally and stained with H&E. A, representative microscopic appearance of colonic ulcers in PBS- and HGF-treated rats. In TNBS-induced colitis rats treated with PBS, extensive mucosal damage and marked inflammatory cell infiltration were observed on day 10. Treatment with recombinant HGF enhanced the development of regenerative epithelium and reduced inflammatory cell infiltrates and edema (magnifications, ×100). B, blind histologic scoring was performed. Rats treated with PBS had a higher histologic score than those treated with recombinant human HGF (*, $P = 0.030$). C, MPO activity in the normal (N) or TNBS-inflamed colon tissues (n = 3 or 4, respectively) was measured. Colonic MPO activity observed on day 10 in rats with TNBS-induced colitis was significantly higher than in normal rats (*, $P = 0.0009$). HGF treatment significantly reduced the MPO activity in rats with TNBS-induced colitis (**, $P = 0.0013$).

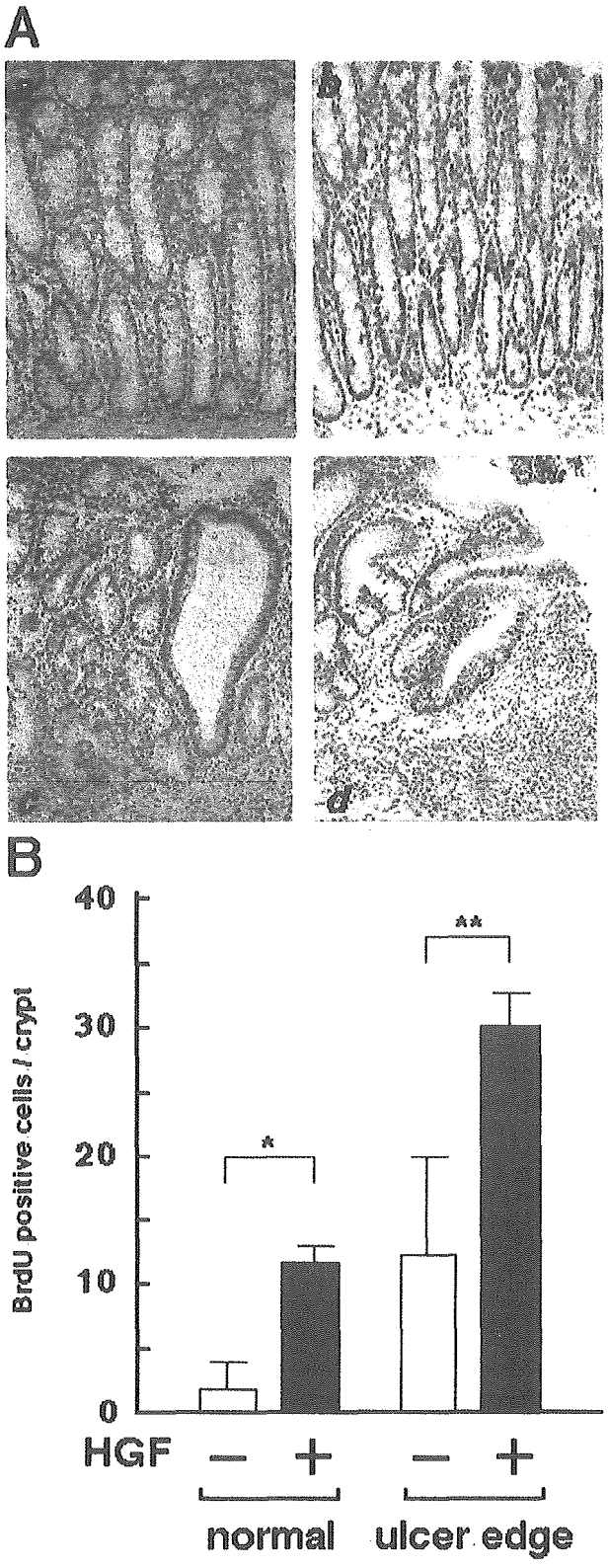


tissues was reduced to 36.8 ± 9.7 pg/mg; however, the difference was not significant ($P = 0.067$).

## DISCUSSION

In this animal model of TNBS-induced colitis, granulomas with inflammatory cell infiltrates in all layers were visible in the intestine.[25] Isolated macrophages produce large amount of interleukin (IL)-12, and lymphocytes produce large amounts of IFNγ and IL-2, indicating that the colitis in this model is induced by a T-helper type 1 response.[26] Thus, animals with TNBS-induced colitis are considered an appropriate model for Crohn's disease. Susceptibility to TNBS varies in each animal, however, resulting in different colitis levels after a single enema of TNBS. In this study, we performed colonoscopic examinations 5 days after the TNBS enema, and only animals with large colonic ulcers—80% of TNBS-treated rats—were given HGF. Using colonoscopy in living animals, we were able to evaluate not only the severity of colitis, but also the healing process of the injured mucosa. Colonoscopic examination of rodents has been recently reported to be feasible and enables continuous observation of dextran sulfate sodium (DSS)-induced colitis without the need for death.[27,28] Therefore, colonoscopy is advantageous to evaluate the response of injured colonic mucosa to experimental therapeutics.

We have previously reported that the continuous intraperitoneal delivery of recombinant human HGF allows detection of the human HGF in rat serum and successfully stimulates colonic mucosal repair in rats with DSS-induced colitis.[18] Recombinant human HGF circulating in the blood is thought to interact with c-Met, a specific receptor for HGF expressed on the basolateral membranes of intestinal epithelial cells,[29] and this interaction leads to the stimulation of cell migration and proliferation. In this study, daily intravenous bolus injections of recombinant human HGF stimulated the proliferation of colonic epithelial cells and facilitated the repair of the deep and large TNBS-induced colonic ulcers. The healing of deeper, penetrating injuries requires reparative mechanisms involving not only epithelial cells, but also nonepithelial cells, angiogenesis, and scarring responses in the submucosal and

**FIGURE 5.** Proliferation of colonic epithelial cells is stimulated by intravenous administration of recombinant human HGF. A, representative photographs of BrdU immunohistochemistry in normal mucosa (a and b) and that bordering ulcers (c and d) in rats with TNBS-induced colitis, which were administered PBS (a and c) or recombinant HGF (b and d; magnifications, ×400). B, BrdU-positive cells were counted, and the number of positive cells per crypt was calculated. In rats treated with PBS alone (n = 8), BrdU-positive cells in the mucosa-bordering ulcers were increased in comparison with those in the normal mucosa. HGF administration, however, stimulated the proliferation of epithelial cells in both normal and border mucosa (* and **, $P = 0.004$ and 0.047, respectively; n = 9).

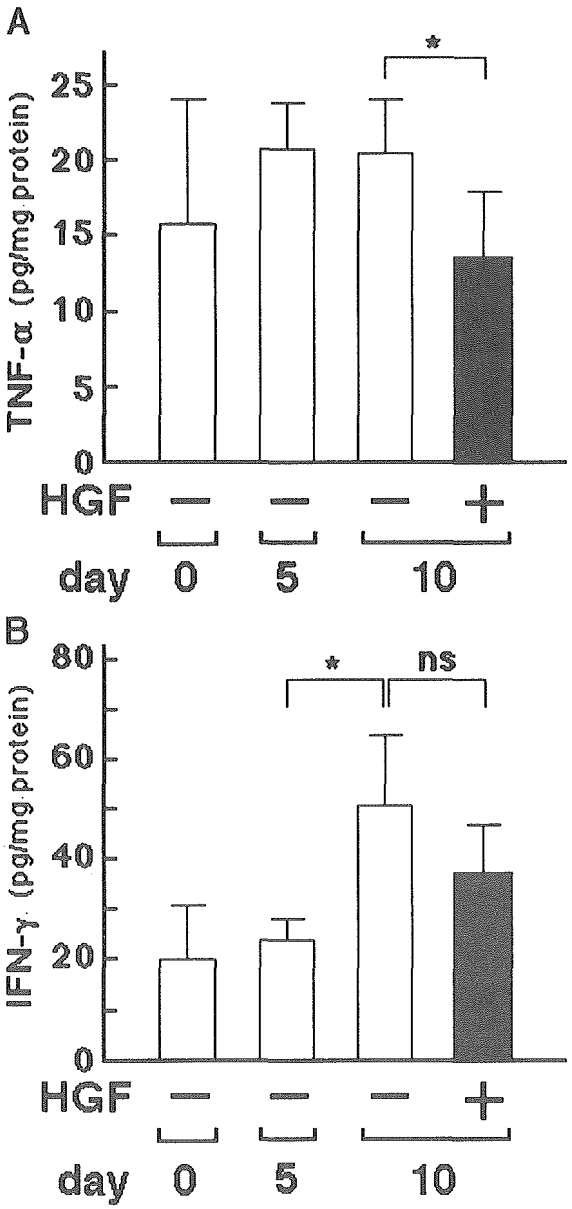


**FIGURE 6.** HGF administration reduces TNFα and IFNγ in colon tissues of rats with TNBS-induced colitis. The levels of TNFα and IFNγ in colon tissues treated with PBS or HGF were determined by ELISA on days 0 (normal rat), 5, and 10 of TNBS administration (n = 4). A, intravenous HGF administration significantly reduced TNFα in colon tissues compared with those in PBS-treated rats on day 10 (*, $P = 0.028$). B, rats given TNBS exhibited a significant increase in IFNγ levels in colon tissues by day 10 (*, $P = 0.003$ compared with those on day 5). The IFNγ levels in colon tissues of HGF-treated rats decreased by day 10. However, these differences were not statistically significant ($P = 0.067$) compared with those of PBS-treated rats.

serosal layers of the intestines. In such a response, angiogenesis is initiated and fibroblasts participate in depositing extracellular matrix components and in shaping the resulting granulated tissue.[30] HGF is known to act not only on epithelial cells, but also on nonepithelial cells (including vascular endothelial cells), and also functions as an angiogenic factor.[31] Therefore, despite the short half-life of the recombinant protein (~2.5 min),[19] intravenous bolus injections of human HGF may effectively ameliorate TNBS-induced colonic ulcers. Additionally, because HGF also acts as an antifibrogenic and angiogenic factor, its administration may potentially suppress development of fibrosis, which causes intestinal stenosis in patients with Crohn's disease.

In injured intestinal tissues, myofibroblasts beneath the epithelial lesion are known to secrete HGF.[3,32,33] Inflammatory cells, such as neutrophils, also produce HGF along with proinflammatory cytokines.[34] Thus, HGF plays a pivotal role in tissue repair. Recently, several groups have reported that HGF induces lymphocyte function-associated antigen-1–mediated adhesion of neutrophils to endothelial cells and also stimulates transmigration of inflammatory cells, including neutrophils and lymphocytes.[35–37] These findings suggest that HGF participates in the activation of the nonspecific cellular inflammatory response in the microenvironment of injured tissues. In this study, although TNBS-induced colitis rats treated with PBS exhibited remarkable infiltration of inflammatory cells, expanding deeply into the large intestinal wall, the inflammatory cell infiltrate and the corresponding increase in proinflammatory cytokines were reduced by treatment with recombinant human HGF. The effect of exogenous HGF on the immune and inflammatory cells in the submucosa remains obscure. However, it is possible that HGF-induced enhancement of mucosal repair allows for a more rapid recovery of epithelial barrier function, leading to a reduced exposure to various luminal agents that contribute to persistent colitis. Therefore, the observed reduction of inflammation in HGF-treated rats may result from a decrease in exposure to luminal stimuli rather than from the direct influence of HGF on immune and inflammatory cells.

We have recently reported that recombinant human HGF, injected intravenously in a bolus, primarily distributes to the liver and that the HGF content in colon tissues is much smaller than in liver, spleen, adrenal glands, and kidneys.[19] We show here that daily intravenous bolus injections of recombinant HGF for 5 days ameliorated large colonic ulcers, despite the small amount of recombinant protein that is supposedly delivered to colonic tissues. c-Met is expressed on basolateral membranes of intestinal epithelial cells,[29] and an increase in recombinant HGF circulating in the blood is therefore considered to stimulate mucosal repair. However, once intestinal mucosal injury occurs, intracellular junctions between epithelial cells are loosened, and the separation, spreading, and migration of epithelial cells are facilitated by the reparative process. This suggests that, compared with

normal mucosa, the distribution of c-Met in epithelial cells is altered. Therefore, luminal administration of recombinant human HGF also has the potential to ameliorate intestinal tissue injury with less adverse side effects, such as renal toxicity.

In conclusion, we performed colonoscopies in living animals to study the various susceptibilities to TNBS in each animal, and we showed that repeated intravenous injections of recombinant human HGF facilitates the repair of large, deep colonic ulcers in a rat model of TNBS-induced colitis. Clarification of the carcinogenic risk will require further study, as will the development of an efficient drug delivery system. However, in contrast to anti-inflammatory or anti-immune agents, recombinant human HGF may be a new modality to eradicate uncontrolled and perpetuated inflammation through enhanced mucosal wound healing in patients with IBD. Additionally, because HGF induces a rapid recovery of the epithelial barrier, HGF treatment may also be more physiological than treatments with anti-inflammatory or anti-immune agents.

## ACKNOWLEDGMENTS

The authors thank Sayoko Ohara, Kana Ohara, and Yuko Nakamura for technical assistance..

## REFERENCES


1. Murphy MS. Growth factors and the gastrointestinal tract. *Nutrition.* 1998;14:771–774.
2. Beck PL, Podolsky DK. Growth factors in inflammatory bowel disease. *Inflamm Bowel Dis.* 1999;5:44–60.
3. Dignass AU, Sturm A. Peptide growth factors in the intestine. *Eur J Gastroenterol Hepatol.* 2001;13:763–770.
4. Gohda E, Tsubouchi H, Nakayama H, et al. Human hepatocyte growth factor in plasma from patients with fulminant hepatic failure. *Exp Cell Res.* 1986;166:139–150.
5. Gohda E, Tsubouchi H, Nakayama H, et al. Purification and partial characterization of hepatocyte growth factor from plasma of a patient with fulminant hepatic failure. *J Clin Invest.* 1988;81:414–419.
6. Igawa T, Kanda S, Kanetake H, et al. Hepatocyte growth factor is a potent mitogen for cultured rabbit renal tubular epithelial cells. *Biochem Biophys Res Commun.* 1991;174:831–838.
7. Joplin R, Hishida T, Tsubouchi H, et al. Human intrahepatic biliary epithelial cells proliferate in vitro in response to human hepatocyte growth factor. *J Clin Invest.* 1992;90:1284–1289.
8. Takahashi M, Ota S, Terano A, et al. Hepatocyte growth factor induces mitogenic reaction to the rabbit gastric epithelial cells in primary culture. *Biochem Biophys Res Commun.* 1993;19:528–534.
9. Dignass AU, Lynch-Devaney K, Podolsky K. Hepatocyte growth factor/scatter factor modulates intestinal epithelial cell proliferation and migration. *Biochem Biophys Res Commun.* 1994;202:701–709.
10. Weidner KM, Sachs M, Birchmeier W. The Met receptor tyrosine kinase transduces motility, proliferation, and morphogenic signals of scatter factor/hepatocyte growth factor in epithelial cells. *J Cell Biol.* 1993;121: 145–154.
11. Kitamura S, Kondo S, Shimomura Y, et al. Expression of hepatocyte growth factor and c-met in ulcerative colitis. *Inflamm Res.* 2000;49:320–324.
12. Matsuo M, Shiota G, Umeki K, et al. Induction of plasma hepatocyte growth factor in acute colitis of mice. *Inflamm Res.* 1997;46:166–167.
13. Ortega-Cava CF, Ishihara S, Kawashima K, et al. Hepatocyte growth factor expression in dextran sodium sulfate-induced colitis in rats. *Dig Dis Sci.* 2002;47:2275–2285.
14. Itoh H, Kataoka H, Tomita M, et al. Upregulation of HGF activator inhibitor type 1 but not type 2 along with regeneration of intestinal mucosa. *Am J Physiol Gastrointest Liver Physiol.* 2000;278:G635–G643.
15. Kataoka H, Shimomura T, Kawaguchi T, et al. Hepatocyte growth factor activator inhibitor type 1 is a specific cell surface binding protein of hepatocyte growth factor activator (HGFA) and regulates HGFA activity in the pericellular microenvironment. *J Biol Chem.* 2000;275: 40453–40462.
16. Hanauer SB, Present DH. The state of the art in the management of inflammatory bowel disease. *Rev Gastroenterol Disord.* 2003;3:81–92.
17. Sandborn WJ, Hanauer SB. Antitumor necrosis factor therapy for inflammatory bowel disease: a review of agents, pharmacology, clinical results, and safety. *Inflamm Bowel Dis.* 1999;5:119–133.
18. Tahara Y, Ido A, Yamamoto S, et al. Hepatocyte growth factor facilitates colonic mucosal repair in experimental ulcerative colitis in rats. *J Pharm Exp Therap.* 2003;307:146–151.
19. Ido A, Moriuchi A, Kim IL, et al. Pharmacokinetic study of recombinant human hepatocyte growth factor administered in a bolus intravenously or via portal vein. *Hepatol Res.* 2004;30:175–181.
20. Stucchi AF, Shofer S, Leeman S, et al. NK-1 antagonist reduces colonic inflammation and oxidative stress in dextran sulfate-induced colitis in rats. *Am J Physiol Gastrointest Liver Physiol.* 2000;279:G1298–G1306.
21. Macpherson BR, Pfeiffer CJ. Experimental production of diffuse colitis in rats. *Digestion.* 1978;17:135–150.
22. Tsune I, Ikejima K, Hirose M, et al. Dietary glycine prevents chemical-induced experimental colitis in the rat. *Gastroenterology.* 2003;125:775–785.
23. Bradley PP, Priebat DA, Christensen RD, et al. Measurement of cutaneous inflammation: estimation of neutrophil content with an enzyme marker. *J Invest Dermatol.* 1982;78:206–209.
24. Moreels TG, Nieuwendijk RJ, De Man JG, et al. Concurrent infection with Schistosoma mansoni attenuates inflammation induced changes in colonic morphology, cytokine levels, and smooth muscle contractility of trinitrobenzene sulphonic acid induced colitis in rats. *Gut.* 2004;53:99–107.
25. Hibi T, Ogata H, Sakuraba A. Animal models of inflammatory bowel disease. *J Gastroenterol.* 2002;37:409–417.
26. Neurath MF, Fuss I, Kelsall BL, et al. Antibodies to interleukin 12 abrogate established experimental colitis in mice. *J Exp Med.* 1995;182: 1281–1290.
27. Ahn BK, Ko KH, Oh TY, et al. Efficacy of use of colonoscopy in dextran sulfate sodium induced ulcerative colitis in rats: the evaluation of the effects of antioxidant by colonoscopy. *Int J Colorectal Dis.* 2001;16:174–181.
28. Huang EH, Carter JJ, Whelan RL, et al. Colonoscopy in mice. *Surg Endosc.* 2002;16:22–24.
29. Nusrat A, Parkos CA, Bacarra AE, et al. Hepatocyte growth factor/scatter factor effects on epithelia. Regulation of intercellular junctions in transformed and nontransformed cell lines, basolateral polarization of c-met receptor in transformed and natural intestinal epithelia, and induction of rapid wound repair in a transformed model epithelium. *J Clin Invest.* 1994; 93:2056–2065.
30. Mammen JMV, Matthews JB. Mucosal repair in the gastrointestinal tract. *Crit Care Med.* 2003;31(Suppl):S532–S537.
31. Grant DS, Kleinman HK, Goldberg ID, et al. Scatter factor induces blood vessel formation in vivo. *Proc Natl Acad Sci USA.* 1993;90:1937–1941.
32. Goke M, Kanai M, Podolsky DK. Intestinal fibroblast regulate intestinal epithelial cell proliferation via hepatocyte growth factor. *Am J Physiol Gastrointest Liver Physiol.* 1998;274:G809–G818.
33. Hori T, Ido A, Uto H, et al. Activation of hepatocyte growth factor in monkey stomach following gastric mucosal injury. *J Gastroenterol.* 2004;39: 133–139.
34. Grenier A, Chollet-Martin S, Crestani B, et al. Presence of a mobilizable intracellular pool of hepatocyte growth factor in human polymorphonuclear neutrophils. *Blood.* 2002;99:2997–3004.
35. Adams DH, Harvath L, Bottaro DP, et al. Hepatocyte growth factor and macrophage inflammatory protein 1b: Structurally distinct cytokines that induce rapid cytoskeletal changes and subset-preferential migration in T cells. *Proc Natl Acad Sci USA.* 1994;91:7144–7148.
36. Mine S, Tanaka Y, Suematu M, et al. Hepatocyte growth factor is a potent trigger of neutrophil adhesion through rapid activation of lymphocyte function-associated antigen-1. *Lab Invest.* 1998;78:1395–1404.
37. Beilmann M, Vande Woude GF, Dienes HP, et al. Hepatocyte growth factor-stimulated invasiveness of monocytes. *Blood.* 2000;95: 3964–3969.

nature medicine



# Induction of interleukin-8 preserves the angiogenic response in HIF-1α–deficient colon cancer cells

Yusuke Mizukami[1], Won-Seok Jo[1], Eva-Maria Duerr[1], Manish Gala[1], Jingnan Li[1], Xiaobo Zhang[1], Michael A Zimmer[2], Othon Iliopoulos[2], Lawrence R Zukerberg[3], Yutaka Kohgo[4], Maureen P Lynch[5], Bo R Rueda[5] & Daniel C Chung[1]

**Hypoxia inducible factor-1 (HIF-1) is considered a crucial mediator of the cellular response to hypoxia through its regulation of genes that control angiogenesis[1–4]. It represents an attractive therapeutic target[5,6] in colon cancer, one of the few tumor types that shows a clinical response to antiangiogenic therapy[7]. But it is unclear whether inhibition of HIF-1 alone is sufficient to block tumor angiogenesis[8,9]. In HIF-1α knockdown DLD-1 colon cancer cells (DLD-1$^{HIF\text{-}kd}$), the hypoxic induction of vascular endothelial growth factor (VEGF) was only partially blocked. Xenografts remained highly vascularized with microvessel densities identical to DLD-1 tumors that had wild-type HIF-1α (DLD-1$^{HIF\text{-}wt}$). In addition to the preserved expression of VEGF, the proangiogenic cytokine interleukin (IL)-8 was induced by hypoxia in DLD-1$^{HIF\text{-}kd}$ but not DLD-1$^{HIF\text{-}wt}$ cells. This induction was mediated by the production of hydrogen peroxide and subsequent activation of NF-κB. Furthermore, the *KRAS* oncogene, which is commonly mutated in colon cancer, enhanced the hypoxic induction of IL-8. A neutralizing antibody to IL-8 substantially inhibited angiogenesis and tumor growth in DLD-1$^{HIF\text{-}kd}$ but not DLD-1$^{HIF\text{-}wt}$ xenografts, verifying the functional significance of this IL-8 response. Thus, compensatory pathways can be activated to preserve the tumor angiogenic response, and strategies that inhibit HIF-1α may be most effective when IL-8 is simultaneously targeted.**

We subcutaneously injected DLD-1 cells, which contained either wild-type HIF-1α or HIF-1α stably knocked down by siRNA[10] (DLD-1$^{HIF\text{-}wt}$ or DLD-1$^{HIF\text{-}kd}$, respectively), into CD1 nude mice. Four weeks after inoculation, tumor volumes and weights were significantly lower in DLD-1$^{HIF\text{-}kd}$ tumors (**Fig. 1a,b**), indicating an important role for HIF-1 in tumor growth *in vivo*. We confirmed this finding in an independent colon cancer cell line, Caco2 (**Supplementary Fig. 1** online). Large necrotic areas were much more prevalent in DLD-1$^{HIF\text{-}wt}$ xenografts (**Fig. 1c**). Furthermore, a prominent inflammatory infiltrate composed predominantly of neutrophils was observed only in DLD-1$^{HIF\text{-}kd}$ xenografts (**Fig. 1c**). Although there were larger areas of necrosis in DLD-1$^{HIF\text{-}wt}$ xenografts, the cross-sectional surface area of non-necrotic viable tumor was still significantly greater when compared to DLD-1$^{HIF\text{-}kd}$ xenografts (0.33 $cm^2$ versus 0.16 $cm^2$, respectively, $P = 0.025$). Thus, the difference in size of the tumors cannot be entirely attributed to the larger area of necrosis in the DLD-1$^{HIF\text{-}wt}$ tumors. A persistent silencing effect of the HIF-1α siRNA construct was confirmed *in vivo* (**Fig. 1d**).

There was a significant decrease in the Ki-67 labeling index in DLD-1$^{HIF\text{-}kd}$ xenografts (41.3 ± 3.2% in DLD-1$^{HIF\text{-}wt}$ tumors versus 27.4 ± 2.6% in DLD-1$^{HIF\text{-}kd}$ tumors; $P < 0.01$), suggesting that HIF-1α regulates cellular proliferation *in vivo*. We calculated the apoptotic index by counting TUNEL-positive cells in non-necrotic areas. We observed a small but statistically significant difference in the apoptotic index between the two groups (3.2 ± 0.53% in DLD-1$^{HIF\text{-}wt}$ tumors versus 1.9 ± 0.42% in DLD-1$^{HIF\text{-}kd}$ tumors; $P < 0.05$), but this difference is unlikely to counterbalance the considerable difference in proliferation rates.

When we incubated DLD-1$^{HIF\text{-}kd}$ cells under hypoxic conditions (1% $O_2$) *in vitro*, we observed only a 25% reduction ($P = 0.11$) in the induced levels of *VEGF* mRNA and protein (**Fig. 1e**). In the DLD-1$^{HIF\text{-}kd}$ xenografts, *VEGF* mRNA and protein levels were also induced (**Fig. 1f**), though not to the same extent observed *in vitro*. Compared to the DLD-1$^{HIF\text{-}wt}$ xenografts, *VEGF* mRNA levels were 51% lower ($P = 0.028$) and protein levels were 52% lower ($P = 0.0024$) in DLD-1$^{HIF\text{-}kd}$ xenografts. This persistent expression of VEGF was not mediated by HIF-2α, as mRNA encoding HIF-2α and HIF-2α protein levels were barely detectable in normoxic conditions and the gene was not induced by hypoxia (**Supplementary Fig. 2** online).

To specifically address whether hypoxia regulates VEGF in the absence of HIF-1 *in vivo*, we identified hypoxic areas within the tumor mass using Hypoxyprobe-1 (pimonidazole hydroxychloride). There were large hypoxic regions surrounding the necrotic areas in the center of the DLD-1$^{HIF\text{-}wt}$ tumors (**Fig. 1g**). In contrast, DLD-1$^{HIF\text{-}kd}$ tumors showed only restricted regions of intratumoral hypoxia. Double immunofluorescence showed that VEGF was preferentially

[1]Gastrointestinal Unit, [2]Oncology Unit, Department of Medicine and [3]Department of Pathology, Massachusetts General Hospital and Harvard Medical School, 50 Blossom Street, Boston, Massachusetts 02114, USA. [4]Third Department of Internal Medicine, Asahikawa Medical College, 2-1 Midorigaoka-Higashi, Asahikawa, 078-8510 Japan. [5]Vincent Center for Reproductive Biology, Department of Obstetrics and Gynecology, Massachusetts General Hospital and Harvard Medical School, 50 Blossom Street Boston, Massachusetts 02114, USA. Correspondence should be addressed to D.C.C. (chung.daniel@mgh.harvard.edu).

Published online 28 August 2005; doi:10.1038/nm1294

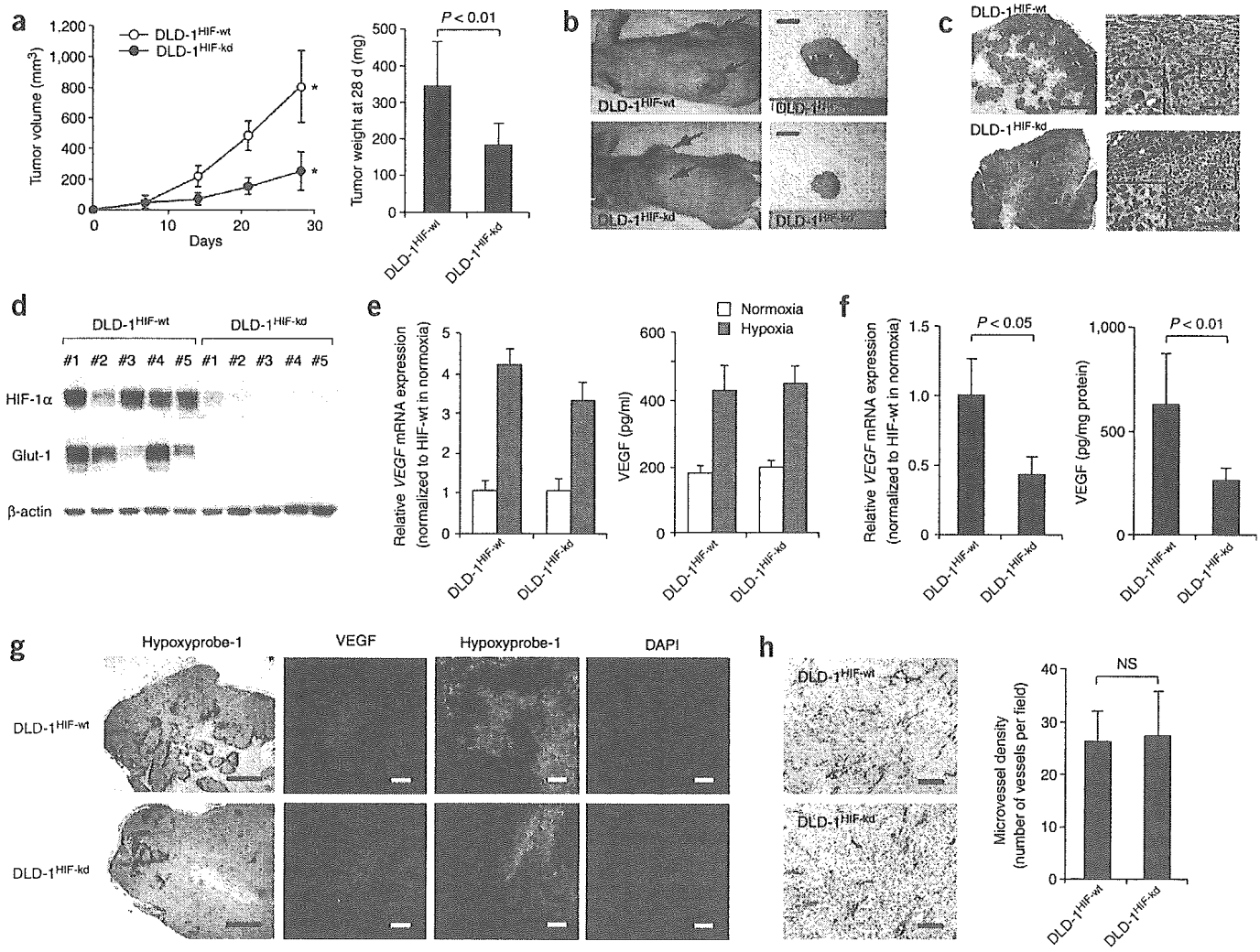


**Figure 1** Growth of DLD-1$^{HIF\text{-}kd}$ cells *in vivo*. (**a**) Tumor volume and weight of DLD-1$^{HIF\text{-}wt}$ and DLD-1$^{HIF\text{-}kd}$ xenografts. *$P < 0.05$. (**b**) Gross appearance of xenografts and excised tumors at 4 weeks. Scale bar, 5 mm. (**c**) H&E staining of resected tumors. Left scale bars, 1 mm; right scale bars, 50 μm. (**d**) Immunoblotting for HIF-1α and Glut-1 in DLD-1$^{HIF\text{-}kd}$ xenografts. *VEGF* mRNA and protein levels in cultured DLD-1 cells (**e**) and in tumor xenografts (**f**) were measured. (**g**) Intratumoral 'hypoxia' was detected by immunohistochemistry for Hypoxyprobe-1. Scale bar, 1 mm. Immunofluorescent staining for VEGF (Texas red) and Hypoxyprobe-1 (FITC). Scale bar, 100 μm. (**h**) Immunohistochemistry for CD31 and quantification of microvessel density in DLD-1 xenografts. Scale bar, 100 μm.

expressed in the hypoxic areas of both DLD-1$^{HIF\text{-}kd}$ and DLD-1$^{HIF\text{-}wt}$ xenografts (**Fig. 1g**).

It is possible that the difference in growth between the xenografts resulted from impaired angiogenesis, potentially attributable to lower levels of VEGF in DLD-1$^{HIF\text{-}kd}$ tumors. But immunostaining for the endothelial cell marker CD31 showed abundant microvascular networks in all tumors (**Fig. 1h**). We observed no quantitative difference in microvessel density (26.1 ± 6.3/field in DLD-1$^{HIF\text{-}wt}$ and 28.7 ± 8.6/field in DLD-1$^{HIF\text{-}kd}$ xenografts), suggesting that high levels of HIF-1 may not be required to stimulate angiogenesis or maintain vessel integrity in DLD-1 tumors.

Although upregulation of VEGF was preserved in DLD-1$^{HIF\text{-}kd}$ xenografts, the absolute levels of VEGF were reduced. We therefore determined whether other angiogenic factors may be induced in a compensatory manner to maintain tumor vascularity in the absence of HIF-1. cDNA microarray analysis identified genes that were upregulated at least twofold by hypoxia but whose expression was attenuated less than 30% when HIF-1 was silenced. *VEGF* was upregulated fourfold in DLD-1$^{HIF\text{-}wt}$ cells by hypoxia, and this induction was decreased only 10.6% by HIF-1 silencing (**Supplementary Table 1** online). In addition, expression of the proangiogenic cytokine *IL-8* was increased twofold in DLD-1$^{HIF\text{-}kd}$ cells cultured in hypoxic conditions compared to DLD-1$^{HIF\text{-}wt}$ cells.

Hypoxia upregulated *IL-8* mRNA >2.5-fold in DLD-1$^{HIF\text{-}kd}$ cells, but there was no induction in DLD-1$^{HIF\text{-}wt}$ cells (**Fig. 2a**). Consistent with this result, the level of IL-8 in the supernatant of DLD-1$^{HIF\text{-}kd}$ cells was increased almost threefold compared to DLD-1$^{HIF\text{-}wt}$ cells. We obtained similar results with previously established, independent DLD-1$^{HIF\text{-}kd}$ clones[10] (data not shown). Extracts from DLD-1$^{HIF\text{-}kd}$ xenografts also showed significantly higher *IL8* mRNA and protein levels when compared to DLD-1$^{HIF\text{-}wt}$ tumors (**Fig. 2b**). *IL-8* promoter reporter constructs showed higher basal activity in DLD-1$^{HIF\text{-}kd}$ cells (**Fig. 2c**), and there was further induction of promoter activity in hypoxia that was not observed in the DLD-1$^{HIF\text{-}wt}$ cells. There was also a 2.1-fold induction of the *IL-8* promoter when HIF-1α was transiently knocked down in parental DLD-1 cells, indicating this

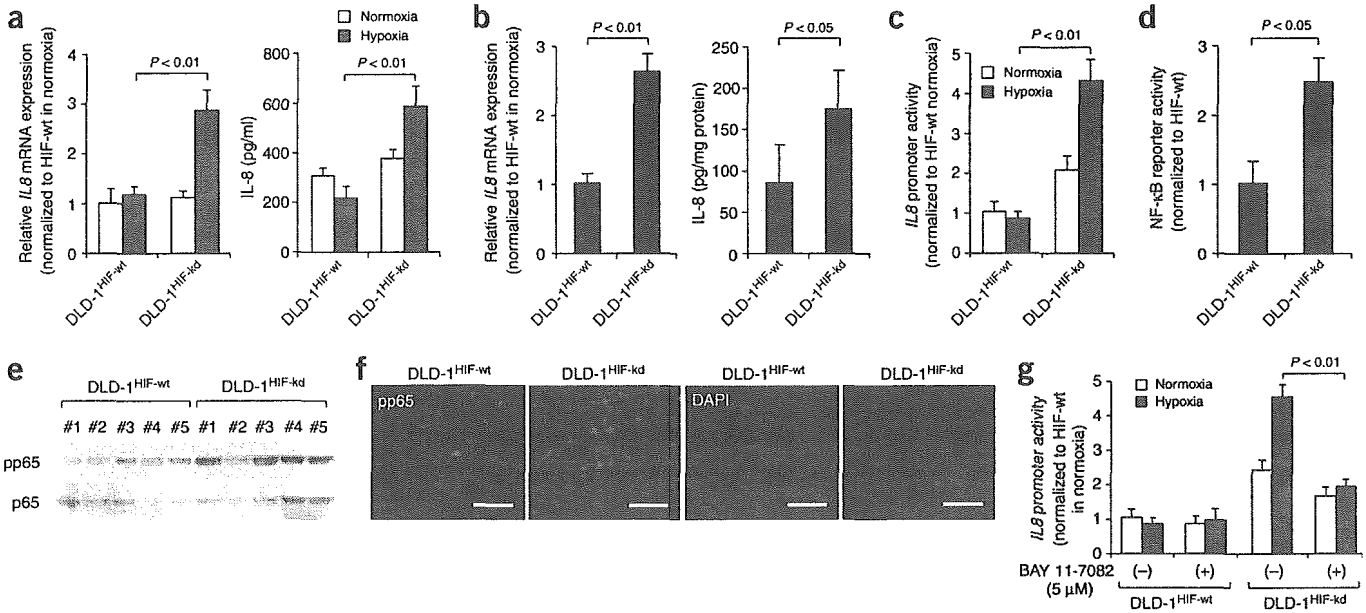


**Figure 2** *Knockdown of HIF-1 facilitates the induction of IL-8 by NF-κB during hypoxic conditions. IL8 mRNA and protein levels in* (**a**) cultured DLD-1 cells and (**b**) DLD-1 xenografts. (**c**) *IL8* promoter activity during hypoxia in DLD-$1^{HIF\text{-}kd}$ and DLD-$1^{HIF\text{-}wt}$ cells. (**d**) NF-κB reporter activity in hypoxic conditions in DLD-$1^{HIF\text{-}kd}$ cells. (**e**) Immunoblotting for NF-κB, p65 subunit and Ser536-phosphorylated p65 (p-p65), in DLD-1 tumor lysates. (**f**) Immunohistochemistry for phosphorylated p65 in DLD-1 xenografts (shown as Texas Red). Scale bar, 50 μm. (**g**) Effect of NF-κB inhibition on *IL8* promoter activity with BAY 11-7082.



phenomenon was not an artifact of the stable transfection process. In addition, expression of a constitutively active HIF-1α in which the proline at position 564 was changed to an alanine in DLD-1 cells did not induce the *IL-8* promoter (1.01 ± 0.14-fold increase), indicating that HIF-1 does not directly regulate *IL-8* gene expression. This hypoxic effect was not unique to DLD-1 cells. Knockdown of HIF-1α in additional colon cancer cells (ColoHSR, SW 480 and HCT116), pancreatic cancer cells (Panc-1, CAPAN-1), breast cancer cells (MDA-MB-453) and lung cancer cells (HOP-92) showed a similar induction of IL-8 in hypoxia (**Supplementary Fig. 3** online). Finally, we confirmed specificity of these siRNA constructs by observing expression of HIF-1α synonymous codon mutants (**Supplementary Fig. 4** online). The absence of HIF-1 can therefore stimulate IL-8 on a transcriptional level, and this is further enhanced in hypoxia.

NF-κB is a major regulator of IL-8. NF-κB reporter activity was increased 151% ($P < 0.01$) in HIF-1α knockdown cells (**Fig. 2d**). Western blotting (**Fig. 2e**) and immunohistochemistry (**Fig. 2f**) of tissue xenografts showed that phosphorylation of the p65 subunit was greater in DLD-$1^{HIF\text{-}kd}$ xenografts, suggesting that HIF-1 inhibition does upregulate the NF-κB pathway *in vivo*. Densitometry of western blots quantified a 2.0 ± 0.4-fold increase in the ratio of phosphorylated p65 to unphosphorylated p65 ($P < 0.01$). The hypoxic induction of the *IL-8* promoter in DLD-$1^{HIF\text{-}kd}$ cells was significantly downregulated by BAY 11-7082, a specific inhibitor of NF-κB[11] (**Fig. 2g**). Thus, activation of the NF-κB pathway is important for the induction of IL-8 in the absence of HIF-1.

We then speculated that HIF-1 inhibition may enhance the production of hydrogen peroxide ($H_2O_2$), a reactive oxygen species (ROS) that can activate NF-κB[12,13]. Hypoxic conditions can lead to the increased production of ROS[14,15], and scavenging of ROS is often achieved by increased production of pyruvate[16] that occurs when cells shift from oxidative to glycolytic metabolism. This shift depends upon HIF-1α[17]. DLD-$1^{HIF\text{-}kd}$ cells released more $H_2O_2$ *in vitro*, and hypoxia further enhanced its production (**Fig. 3a**). Four distinct chemical inhibitors of ROS production (*N*-acetyl-L-cysteine, pyrrolidinedithiocarbamate, rotenone and diphenylene iodonium) each strongly blocked the induction of NF-κB promoter activity by hypoxia in DLD-$1^{HIF\text{-}kd}$ cells (**Fig. 3b**). Finally, exogenous administration of the long-acting $H_2O_2$ analog, *t*-butyl hydroperoxide, stimulated the production of IL-8 in parental DLD-1 cells. This induction was inhibited by BAY 11-7082 (**Fig. 3c**), again showing that NF-κB mediates this effect of ROS.

In contrast to DLD-$1^{HIF\text{-}kd}$ cells, we did not observe hypoxic induction of *IL8* mRNA (**Fig. 3d**) and protein (data not shown) in Caco$2^{HIF\text{-}kd}$ colon cancer cells[10]. Given that DLD-1 cells harbor the Gly13Asp mutation in the *KRAS* oncogene (*KRAS*38g→a), whereas Caco2 cells are wild-type ($KRAS^{35g/35g}$), we speculated that oncogenic *KRAS* may have a role in the hypoxic induction of IL-8 (ref. 18). When we induced the expression of the Gly12Val *KRAS* mutation (KRAS35g→t) in Caco$2^{HIF\text{-}kd}$ cells , hypoxia upregulated *IL-8* mRNA 2.5-fold, whereas the effect was not observed in Caco$2^{HIF\text{-}wt}$ cells or in Caco$2^{HIF\text{-}kd}$ cells exposed to hypoxia only (**Fig. 3d**). $KRAS^{35t}$ only modestly induced *IL-8* mRNA in Caco$2^{HIF\text{-}kd}$ cells in normoxic conditions. Expression of $KRAS^{35t}$ in Caco$2^{HIF\text{-}wt}$ cells also upregulated the *IL-8* promoter, but this activation was more pronounced in Caco$2^{HIF\text{-}kd}$ cells under conditions of hypoxia (**Fig. 3e**). BAY 11-7082 blocked the induction of the *IL-8* promoter by hypoxia and $KRAS^{35t}$ (**Fig. 3e**).

Exogenous expression of oncogenic *KRAS* may act supraphysiologically. Endogenous $KRAS^{38a}$ in DLD-1 cells was therefore silenced by siRNA and this resulted in a 50% reduction of KRAS protein levels, consistent with a silencing effect of the one mutant allele[19]. Knockdown of $KRAS^{38a}$ attenuated the hypoxic induction of an NF-κB reporter and *IL8* promoter activity (**Fig. 3f**) as well as *IL8* mRNA levels (**Fig. 3g**) in DLD-$1^{HIF\text{-}kd}$ but not in DLD-$1^{HIF\text{-}wt}$ cells. These observations were confirmed in the Panc-1 pancreatic and PC3 prostate cancer cell lines, indicating the broader importance of *KRAS* on this alternative regulation of IL-8 (**Supplementary Fig. 5**

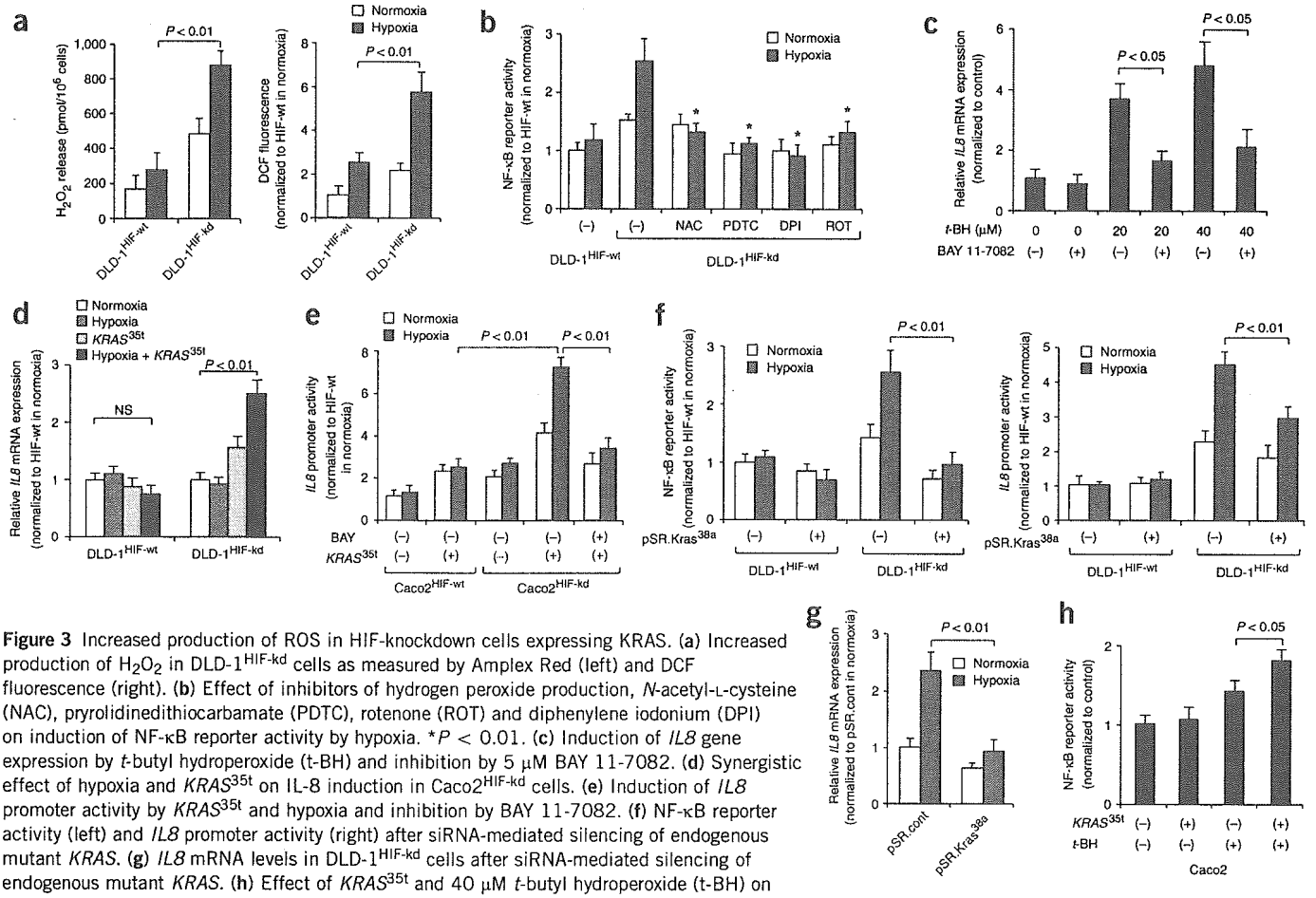


**Figure 3** Increased production of ROS in HIF-knockdown cells expressing KRAS. (**a**) Increased production of $H_2O_2$ in DLD-$1^{HIF\text{-}kd}$ cells as measured by Amplex Red (left) and DCF fluorescence (right). (**b**) Effect of inhibitors of hydrogen peroxide production, *N*-acetyl-L-cysteine (NAC), pyrolidinedithiocarbamate (PDTC), rotenone (ROT) and diphenylene iodonium (DPI) on induction of NF-κB reporter activity by hypoxia. $^*P < 0.01$. (**c**) Induction of *IL8* gene expression by *t*-butyl hydroperoxide (t-BH) and inhibition by 5 μM BAY 11-7082. (**d**) Synergistic effect of hypoxia and $KRAS^{35t}$ on IL-8 induction in Caco$2^{HIF\text{-}kd}$ cells. (**e**) Induction of *IL8* promoter activity by $KRAS^{35t}$ and hypoxia and inhibition by BAY 11-7082. (**f**) NF-κB reporter activity (left) and *IL8* promoter activity (right) after siRNA-mediated silencing of endogenous mutant *KRAS*. (**g**) *IL8* mRNA levels in DLD-$1^{HIF\text{-}kd}$ cells after siRNA-mediated silencing of endogenous mutant *KRAS*. (**h**) Effect of $KRAS^{35t}$ and 40 μM *t*-butyl hydroperoxide (t-BH) on NF-κB reporter activity in Caco2 cells.

online). Furthermore, we observed the stimulatory effect of oncogenic *KRAS* on NF-κB in hypoxic conditions or in the presence of ROS (**Figs. 3d,h**). Collectively, these studies indicate that IL-8 can be induced in hypoxia through the activation of NF-κB in the absence of HIF-1, and that oncogenic *KRAS* can further stimulate NF-κB in hypoxic conditions to upregulate this alternative angiogenic pathway.

Finally, we sought to determine the functional significance of IL-8 production in HIF-1–deficient tumors. The observation that DLD-$1^{HIF\text{-}kd}$ xenografts showed a marked inflammatory infiltrate (**Fig. 1c**) was consistent with a functional role for IL-8, a potent neutrophil chemokine[18]. Intraperitoneal administration of the IL-8 neutralizing antibody MAB208 resulted in complete regression of 25% of DLD-$1^{HIF\text{-}kd}$ xenografts, and among the other detectable DLD-$1^{HIF\text{-}kd}$ tumors, there was a 61.3% reduction in tumor volume ($P < 0.01$) and 61.8% reduction in tumor weight ($P < 0.01$) compared to tumors treated with control IgG (**Fig. 4a,b**). In contrast, there was only a 24.8% ($P = 0.28$) and 15.6% ($P = 0.35$) reduction in tumor volume and weight, respectively, in DLD-$1^{HIF\text{-}wt}$ xenografts. Although treatment with MAB208 resulted in a decrease in the Ki-67 labeling index and increase in apoptosis in the DLD-$1^{HIF\text{-}kd}$ xenografts (**Fig. 4c**), *in vitro* studies showed that MAB208 did not directly inhibit tumor cell growth (**Fig. 4d**). Rather, treatment with MAB208 resulted in a considerable inhibition of angiogenesis. The microvessel density in DLD-$1^{HIF\text{-}kd}$ xenografts was reduced 46.5% ($P < 0.001$) compared to a 14.5% reduction ($P = 0.11$) in DLD-$1^{HIF\text{-}wt}$ xenografts (**Fig. 4e**). Confocal microscopy of tumor sections after lectin perfusion verified that vascular integrity was compromised in DLD-$1^{HIF\text{-}kd}$ xenografts treated with MAB208 (**Fig. 4e**). In addition to reduced vessel number, the vessels were markedly narrowed and fragmented. Specifically, the mean vessel diameter fell from 22.4 μm to 5.9 μm ($P = 0.0002$) when we treated DLD-$1^{HIF\text{-}kd}$ xenografts with MAB208, but there was no change in the DLD-$1^{HIF\text{-}wt}$ xenografts (26.5 μm versus 24.8 μm with MAB208; not significant). Neutralization of both IL-8 and VEGF in DLD-$1^{HIF\text{-}kd}$ xenografts had an additive effect on the inhibition of tumor growth (**Fig. 4f**), showing that each factor can regulate tumorigenesis independently.

In summary, we have shown that HIF-1α deficiency in colon cancer cells can inhibit proliferation and overall growth, but not angiogenesis. There are conflicting reports of the role of HIF-1 in tumor cell proliferation. *Hif1a*$^{-/-}$ embryonic stem cell–derived teratocarcinomas show reduced as well as increased growth[2,20]. Among human tumors, overexpression of HIF-1α has been associated with improved survival in individuals with head and neck cancers[21] and HIF-1 can inhibit the growth of renal carcinoma cells[22]. This may be mediated through the induction of the cell-cycle inhibitors p21 and p27 (ref. 23). It has been speculated that HIF-1 may have intrinsic functions to either promote or inhibit tumor growth that depends upon the cellular context[24]. The preservation of angiogenesis in our model can be explained by persistent expression of VEGF as well as induction of the proangiogenic factor, IL-8. IL-8 was stimulated by ROS-mediated activation of NF-κB, and this was enhanced by oncogenic *KRAS*. Neutralization of IL-8 in HIF-1–deficient tumors led to a substantial inhibition of

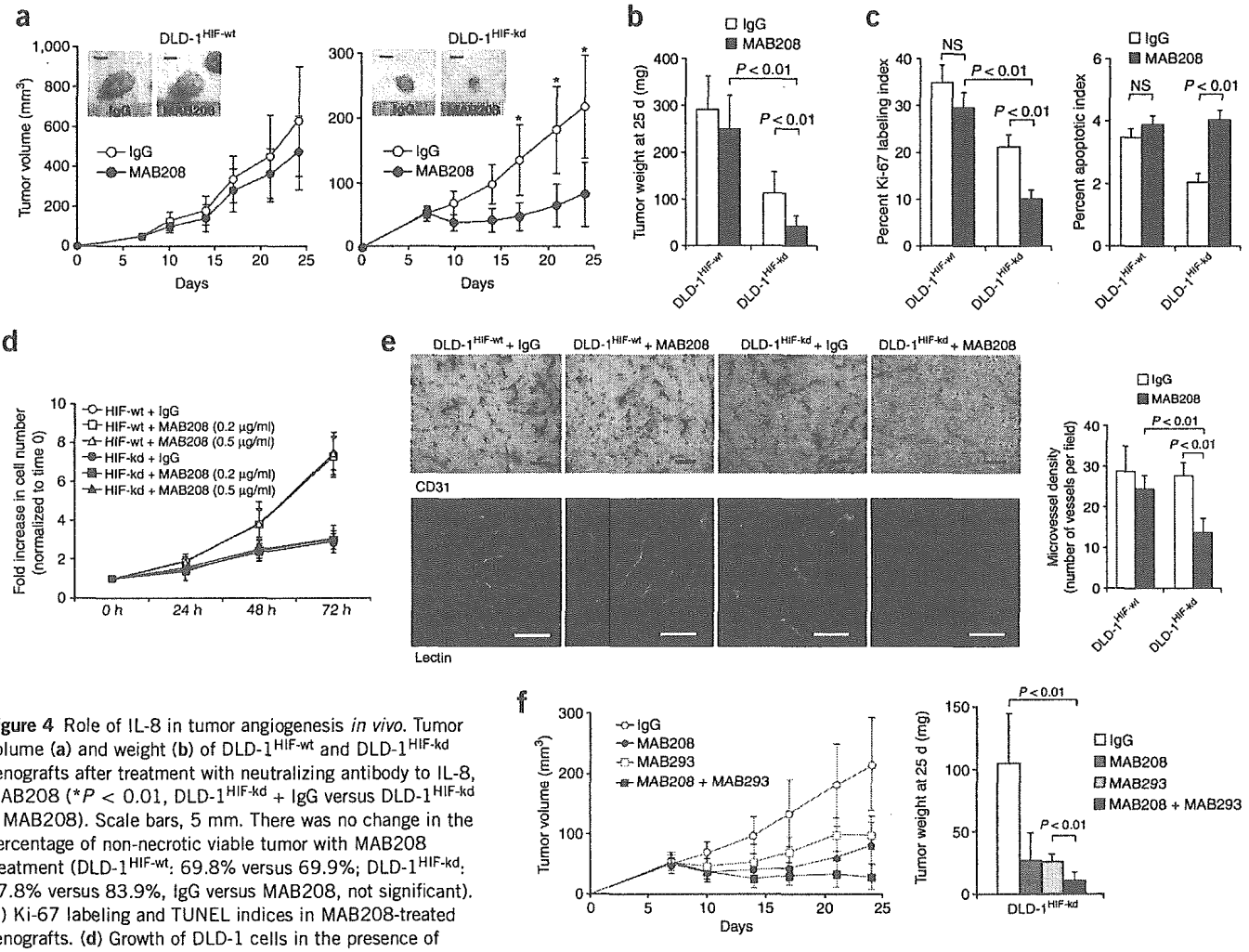


**Figure 4** Role of IL-8 in tumor angiogenesis *in vivo*. Tumor volume (**a**) and weight (**b**) of DLD-1$^{HIF\text{-}wt}$ and DLD-1$^{HIF\text{-}kd}$ xenografts after treatment with neutralizing antibody to IL-8, MAB208 (*$P < 0.01$, DLD-1$^{HIF\text{-}kd}$ + IgG versus DLD-1$^{HIF\text{-}kd}$ + MAB208). Scale bars, 5 mm. There was no change in the percentage of non-necrotic viable tumor with MAB208 treatment (DLD-1$^{HIF\text{-}wt}$: 69.8% versus 69.9%; DLD-1$^{HIF\text{-}kd}$: 87.8% versus 83.9%, IgG versus MAB208, not significant). (**c**) Ki-67 labeling and TUNEL indices in MAB208-treated xenografts. (**d**) Growth of DLD-1 cells in the presence of MAB208 under hypoxic conditions. (**e**) Blood vessels visualized by CD31 immunohistochemistry (upper; scale bar, 100 μm) and lectin perfusion (lower; scale bar, 50 μm). Narrow and fragmented vessels are present in DLD-1$^{HIF\text{-}kd}$ + MAB208. (**f**) Growth of DLD-1$^{HIF\text{-}kd}$ xenografts when treated with a neutralizing VEGF antibody (MAB293) and/or a neutralizing antibody to IL-8 (MAB208). In these xenografts, the percentage of viable non-necrotic tumor fell slightly to 74.7% from 87.8% in mice that received control antibody only ($P = 0.1$).



angiogenesis and tumor growth. Studies of lung cancer cells harboring a *KRAS* mutation have also shown a pivotal role for IL-8 in tumor angiogenesis[25]. Collectively, these findings highlight the complex role of HIF-1α in colorectal tumorigenesis, the diversity of pathways used by tumors to stimulate angiogenesis, and the potential for combination antiangiogenic regimens that target both HIF-1 and IL-8.

## METHODS

**Cell lines.** We stably transfected DLD-1 and Caco2 cells (ATCC) with HIF-1α–specific siRNA constructs (pSuper.retro, OligoEngine), pSR.HIF-1α1470 or pSR.HIF-1α2192 (ref. 10). Three independent DLD-1 clones stably expressing pSR.HIF-1α1470 and two independent clones expressing pSR.HIF-1α2192 showed similar responses to hypoxia with respect to induction of NF-κB and IL-8. In a pilot xenograft study, growth, microvascular density, VEGF and IL-8 levels were similar between a pSR.HIF-1α1470 clone and pSR.HIF-1α2192 clone. Hypoxic conditions (1% $O_2$) were achieved with a sealed hypoxia chamber (Billups-Rothenberg) in serum-free UltraCulture medium (Cambrex)[10]. We performed transient transfections using Lipofectamine 2000 (Invitrogen).

**Plasmid constructs.** The IL-8 reporter[26], NF-κB reporter and phr-GFP-KRAS$^{35t}$ plasmids have been described[27]. We performed site-directed mutagenesis to obtain the phr-GFP-KRAS$^{38a}$ construct. We constructed pSuper.Kras$^{38a}$ (pSR.Kras$^{38a}$) by subcloning the sequence 5′-GGAGCTGGTGACGTAGGCA-3′. For control siRNA, pSR.cont, we used the sequence 5′-GCGCGCTTTGTAG GATTCG-3′ (ref. 28). For mutations in *KRAS*, we used a numbering system in which position 1 is the A of the initiator ATG codon. *KRAS*$^{38a}$ results in a Gly13Asp mutation and *KRAS*$^{35t}$ results in a Gly12Val mutation.

**Transfections and reporter assays.** We cotransfected 0.1–0.2 μg of reporter constructs with 2 ng of pRL-CMV (Promega) and measured luciferase activity with the Dual Luciferase Reporter Assay System (Promega). We used pRL-null, a promoter-less *Renilla* construct, when we cotransfected cells with a KRAS expression vector[29]. We calculated the relative luciferase activity as the ratio of firefly/*Renilla* luciferase activity. The level of 'hypoxic induction' was the ratio between the relative luciferase activity in hypoxia to that in normoxia.

**Xenograft tumor model.** We injected 2 × $10^6$ cells subcutaneously into the flanks of 6–8-week-old CD1 female nude mice (six mice per arm). We measured tumors with calipers and calculated volume as (length × width$^2$) × 0.5. We intraperitoneally administered neutralizing antibody to IL-8 (MAB208, clone 6217.111; R&D Systems) and/or VEGF (MAB293, R&D Systems) when tumors reached 5 mm. We injected 100 μg of MAB208 and/or 25 μg of MAB293 on days 7, 9, 11, 14, 16, 18, 21 and 23, before mice were

killed at day 25. To assess hypoxic regions, we intraperitoneally injected mice with 60 mg/kg pimonidazol hydrochloride (Hypoxyprobe-1, Chemicon), 1.5 h before killing. To visualize functional tumor microvessels, we intravenously injected 100 μg FITC-labeled tomato lectin (Vector Laboratories), and perfused the hearts of the mice with 4% paraformaldehyde. This protocol was approved by the Animal Care and Use Committee of the Massachusetts General Hospital.

**Immunohistochemistry.** We treated 5-μm sections from fresh frozen tumors with acetone and blocked endogenous peroxidase with 3% $H_2O_2$. We incubated the sections with a CD31-specific antibody, MEC13.3 (1:50; Pharmingen), overnight at 4 °C. We counted blood vessels in 5–10 random viable fields (magnification, ×200). To detect tumor hypoxia, we treated formalin-fixed sections with 0.01% pronase and incubated them with Hypoxpyrobe-1–specific antibody Mab1 (1:50; Chemicon). For other immunohistochemical studies, we fixed xenograft tissues in 10% neutral buffered formalin. We performed TUNEL staining with the ApoAlert DNA fragmentation detection kit (Clontech). We performed Ki-67 staining with the MIB-1 antibody (1:100; DAKO) and performed staining for Ser563-phosphorylated p65 (1:50; Cell Signaling).

**Real-time PCR assay.** We extracted RNA using the RNeasy kit (Qiagen) and performed quantitative reverse transcription PCR using the SuperScript III platinum Two-Step qRT-PCR Kit (Invitrogen). Primer sequences for *VEGF*, *IL8* and 18S RNA are available upon request. We used a fluorogenic SYBR Green and MJ research detection system for real-time quantification.

**Immunoblotting.** We performed immunoblot analysis for HIF-1α (clone 54, 1:250; Transduction Laboratories), HIF-2α (1:250, Novus), Glut-1 (GT-11A, 1:1000; Alpha Diagnostic International), VEGF (Ab-2, 1:40; Calbiochem), Ser563-phosphorylated p65 and total NF-κB p65 (1:1,000; both Cell Signaling), KRAS (F234, 1:200; Santa Cruz) and β-actin (AC15, 1 μg/ml; Sigma) after SDS-PAGE and electrophoretic transfer to polyvinylidene fluoride membranes[10].

**ELISA.** We assayed the levels of VEGF and IL-8 protein in conditioned medium and tissue lysates using specific ELISA kits (Quantikine, R&D Systems).

**Microarray analysis.** We performed sample preparation and processing procedures as described in the Affymetrix GeneChip Expression Analysis Manual. We hybridized the labeled cRNA samples to the complete Affymetrix human U133 GeneChip set (HG-U133A).

**Hydrogen peroxide studies.** We measured $H_2O_2$ using the Amplex Red Hydrogen peroxide Assay Kit and the CM-H2DCFDA reagent (both from Molecular Probes). We exposed cells to hypoxia for 10 h, and then switched culture medium to Krebs-Ringer phosphate buffer[30] containing 100 μM Amplex Red reagent and 0.2 U/ml horseradish peroxidase. After additional incubation in hypoxia for 1 h, we measured fluorescence in 96-well plates using Spectra MAX GEMINI XS microplate fluorometer (Molecular Devices). We also incubated cells with 10 μM CM-H2DCFDA for 30 min in RPMI without phenol red. We measured fluorescence in 96-well plates and normalized values to cell number. We added 20 or 40 μM *t*-butyl hydroperoxide (Sigma) to the culture media of DLD-1 cells every 30 min for 6 h and measured *IL8* mRNA using qRT-PCR.

**Statistical analysis.** We performed statistical analyses with a two-tailed, unpaired Student *t*-test.

*Note: Supplementary information is available on the Nature Medicine website.*

ACKNOWLEDGMENTS

We thank the following individuals for sharing these plasmids: C. Reinecker (IL-8 reporter construct), R. Xavier (NF-κB reporter construct, phr-GFP-K-ras$^{Val12}$) and D. Tenen (pRL-null). We also thank Y. Kamegaya, M. Takeda, M. Ii, E. di Tomaso, T. Padera, P. Au and R. Tyszkowski for assistance with tissue analysis. DNA microarray studies were performed at the DNA Microarray Core Facility at the Massachusetts General Hospital Cancer Center. Confocal microscopy was performed through the Imaging Core of the Center for Study of Inflammatory Bowel Diseases. This work was supported by US National Institutes of Health (NIH) research grant CA92594 to D.C.C. O.I. was supported by NIH grant CA104574, B.R.R. was supported by NIH grant CA098333, M.A.Z. was supported by von Hippel-Lindau Family Alliance, M.G. was supported by an American Gastroenterology Association student fellowship award, and E.-M.D. was supported by a postdoctoral fellowship award from the Deutsche Forschungsgemeinschaft.

COMPETING INTERESTS STATEMENT

The authors declare that they have no competing financial interests.

Received 10 June; accepted 2 August 2005
Published online at http://www.nature.com/naturemedicine/

1. Denko, N.C. *et al.* Investigating hypoxic tumor physiology through gene expression patterns. *Oncogene* **22**, 5907–5914 (2003).
2. Carmeliet, P. *et al.* Role of HIF-1alpha in hypoxia-mediated apoptosis, cell proliferation and tumour angiogenesis. *Nature* **394**, 485–490 (1998).
3. Pugh, C.W. & Ratcliffe, P.J. Regulation of angiogenesis by hypoxia: role of the HIF system. *Nat. Med.* **9**, 677–684 (2003).
4. Tang, N. *et al.* Loss of HIF-1alpha in endothelial cells disrupts a hypoxia-driven VEGF autocrine loop necessary for tumorigenesis. *Cancer Cell* **6**, 485–495 (2004).
5. Kung, A.L., Wang, S., Klco, J.M., Kaelin, W.G. & Livingston, D.M. Suppression of tumor growth through disruption of hypoxia-inducible transcription. *Nat. Med.* **6**, 1335–1340 (2000).
6. Semenza, G.L. Targeting HIF-1 for cancer therapy. *Nat. Rev. Cancer* **3**, 721–732 (2003).
7. Hurwitz, H. *et al.* Bevacizumab plus irinotecan, fluorouracil, and leucovorin for metastatic colorectal cancer. *N. Engl. J. Med.* **350**, 2335–2342 (2004).
8. Maxwell, P.H. *et al.* Hypoxia-inducible factor-1 modulates gene expression in solid tumors and influences both angiogenesis and tumor growth. *Proc. Natl. Acad. Sci. USA* **94**, 8104–8109 (1997).
9. Ryan, H.E. *et al.* Hypoxia-inducible factor-1alpha is a positive factor in solid tumor growth. *Cancer Res.* **60**, 4010–4015 (2000).
10. Mizukami, Y. *et al.* Hypoxia-inducible factor-1-independent regulation of vascular endothelial growth factor by hypoxia in colon cancer. *Cancer Res.* **64**, 1765–1772 (2004).
11. Pierce, J.W. *et al.* Novel inhibitors of cytokine-induced IkappaBalpha phosphorylation and endothelial cell adhesion molecule expression show anti-inflammatory effects *in vivo*. *J. Biol. Chem.* **272**, 21096–21103 (1997).
12. Schreck, R., Rieber, P. & Baeuerle, P.A. Reactive oxygen intermediates as apparently widely used messengers in the activation of the NF-kappa B transcription factor and HIV-1. *EMBO J.* **10**, 2247–2258 (1991).
13. Michiels, C., Minet, E., Mottet, D. & Raes, M. Regulation of gene expression by oxygen: NF-kappaB and HIF-1, two extremes. *Free Radic. Biol. Med.* **33**, 1231–1242 (2002).
14. Chandel, N.S. *et al.* Mitochondrial reactive oxygen species trigger hypoxia-induced transcription. *Proc. Natl. Acad. Sci. USA* **95**, 11715–11720 (1998).
15. Chandel, N.S. *et al.* Reactive oxygen species generated at mitochondrial complex III stabilize hypoxia-inducible factor-1alpha during hypoxia: a mechanism of O2 sensing. *J. Biol. Chem.* **275**, 25130–25138 (2000).
16. Brand, K.A. & Hermfisse, U. Aerobic glycolysis by proliferating cells: a protective strategy against reactive oxygen species. *FASEB J.* **11**, 388–395 (1997).
17. Seagroves, T.N. *et al.* Transcription factor HIF-1 is a necessary mediator of the pasteur effect in mammalian cells. *Mol. Cell. Biol.* **21**, 3436–3444 (2001).
18. Sparmann, A. & Bar-Sagi, D. Ras-induced interleukin-8 expression plays a critical role in tumor growth and angiogenesis. *Cancer Cell* **6**, 447–458 (2004).
19. Shirasawa, S., Furuse, M., Yokoyama, N. & Sasazuki, T. Altered growth of human colon cancer cell lines disrupted at activated Ki-ras. *Science* **260**, 85–88 (1993).
20. Ryan, H.E., Lo, J. & Johnson, R.S. HIF-1 alpha is required for solid tumor formation and embryonic vascularization. *EMBO J.* **17**, 3005–3015 (1998).
21. Beasley, N.J. *et al.* Hypoxia-inducible factors HIF-1alpha and HIF-2alpha in head and neck cancer: relationship to tumor biology and treatment outcome in surgically resected patients. *Cancer Res.* **62**, 2493–2497 (2002).
22. Raval, R.R. *et al.* Contrasting properties of hypoxia-inducible factor 1 (HIF-1) and HIF-2 in von Hippel-Lindau-associated renal cell carcinoma. *Mol. Cell. Biol.* **25**, 5675–5686 (2005).
23. Mack, F.A., Patel, J.H., Biju, M.P., Haase, V.H. & Simon, M.C. Decreased growth of Vhl−/− fibrosarcomas is associated with elevated levels of cyclin kinase inhibitors p21 and p27. *Mol. Cell. Biol.* **25**, 4565–4578 (2005).
24. Koshiji, M. & Huang, L.E. Dynamic balancing of the dual nature of HIF-1alpha for cell survival. *Cell Cycle* **3**, 853–854 (2004).
25. Arenberg, D.A. *et al.* Inhibition of interleukin-8 reduces tumorigenesis of human non-small cell lung cancer in SCID mice. *J. Clin. Invest.* **97**, 2792–2802 (1996).
26. Ofori-Darko, E. *et al.* An OmpA-like protein from *Acinetobacter spp.* stimulates gastrin and interleukin-8 promoters. *Infect. Immun.* **68**, 3657–3666 (2000).
27. Khokhlatchev, A. *et al.* Identification of a novel Ras-regulated proapoptotic pathway. *Curr. Biol.* **12**, 253–265 (2002).
28. Zhang, L., Fogg, D.K. & Waisman, D.M. RNA interference-mediated silencing of the S100A10 gene attenuates plasmin generation and invasiveness of Colo 222 colorectal cancer cells. *J. Biol. Chem.* **279**, 2053–2062 (2004).
29. Behre, G., Smith, L.T. & Tenen, D.G. Use of a promoterless Renilla luciferase vector as an internal control plasmid for transient co-transfection assays of Ras-mediated transcription activation. *Biotechniques* **26**, 24–28 (1999).
30. Mohanty, J.G., Jaffe, J.S., Schulman, E.S. & Raible, D.G. A highly sensitive fluorescent micro-assay of H2O2 release from activated human leukocytes using a dihydroxyphenoxazine derivative. *J. Immunol. Methods* **202**, 133–141 (1997).

# CORRIGENDUM: Combating diabetes and obesity in Japan

Y Yazaki & T Kadowaki
*Nat. Med.* **12**, 73–74 (2006)

In **Box 1**, "(BM ≥125)" should read "(BMI ≥25)."

# CORRIGENDUM: ATM regulates target switching to escalating doses of radiation in the intestines

H-J Ch'ang, J G Maj, F Paris, H R Xing, J Zhang, J-P Truman, C Cardon-Cardo, A Haimovitz-Friedman, R Kolesnick & Z Fuchs
*Nat. Med.* **11**, 484–490 (2005)

In **Figure 2a**, ceramide levels at 8 and 12 h after 16 Gy should have read 102 ± 10 and 118 ± 10 percent of control, respectively, and s.e.m. values for the remaining points should be multiplied by a factor of 2.6.

# CORRIGENDUM: Induction of interleukin-8 preserves the angiogenic response in HIF-1α–deficient colon cancer cells

Y Mizukami, W-S Jo, E-M Duerr, M Gala, J Li, X Zhang, M A Zimmer, O Iliopoulos, L R Zukerberg, Y Kohgo, M P Lynch, B R Rueda & D C Chung
*Nat. Med.* **11**, 992–997 (2005)

In **Figure 3d**, the labels for the cell lines are incorrect. Instead of DLD-1/HIF-wt and DLD-1/HIF-kd, the labels should be Caco2/HIF-wt and Caco2/HIF-kd, respectively.

GASTROENTEROLOGY 2005;128:975–986

# Therapeutic Effects of Rectal Administration of Basic Fibroblast Growth Factor on Experimental Murine Colitis

MINORU MATSUURA,* KAZUICHI OKAZAKI,† AKIYOSHI NISHIO,* HIROSHI NAKASE,* HIROYUKI TAMAKI,* KAZUSHIGE UCHIDA,* TOSHIKI NISHI,* MASANORI ASADA,* KIMIO KAWASAKI,* TOSHIRO FUKUI,* HAZUKI YOSHIZAWA,* SHINYA OHASHI,* SATOKO INOUE,* CHIHARU KAWANAMI,* HIROSHI HIAI,§ YASUHIKO TABATA,‖ and TSUTOMU CHIBA*

*Department of Gastroenterology and Endoscopic Medicine, Graduate School of Medicine, §Department of Pathology and Biology of Diseases, and ‖Department of Biomaterials, Institute for Frontier Medical Sciences, Kyoto University, Kyoto; and †Third Department of Internal Medicine, Kansai Medical University, Osaka, Japan

*Background & Aims:* Basic fibroblast growth factor (bFGF) is a promising therapeutic agent for various diseases. It remains unclear, however, whether bFGF is effective for the treatment of inflammatory bowel disease. The aim of this study was to examine the efficacy of bFGF on 2 experimental murine colitis models and to investigate its molecular mechanisms. *Methods:* We evaluated the effects of human recombinant bFGF (hrbFGF) on mice with dextran sulfate sodium (DSS)-induced colitis and mice with trinitrobenzene sulfonic acid (TNBS)-induced colitis as well as normal mice. Body weight, survival rate, and histologic findings of the colonic tissues were examined. Gene expression of tumor necrosis factor (TNF)-α, cyclooxygenase (COX)-2, transforming growth factor (TGF)-β, mucin 2 (MUC2), intestinal trefoil factor (ITF), and vascular endothelial growth factor (VEGF) in the colonic tissues was determined. The proliferation activity of hrbFGF on the colonic epithelium was evaluated by immunohistochemistry. *Results:* Rectal administration of hrbFGF ameliorated DSS-induced colitis in a dose-dependent manner. Gene expression of TNF-α was significantly reduced in the colonic tissues of mice with DSS-induced colitis treated with hrbFGF, whereas MUC2 and ITF messenger RNA expression was up-regulated. Rectal administration of hrbFGF significantly improved the survival rate of mice with TNBS-induced colitis and partially ameliorated colitis. hrbFGF significantly increased the number of Ki-67–positive cells in the colonic epithelium of normal mice, and up-regulated the gene expression of COX-2, TGF-β, MUC2, ITF, and VEGF in the colonic tissues. *Conclusions:* Rectal administration of bFGF might be a promising option for the treatment of inflammatory bowel disease.

Although the cause of inflammatory bowel disease (IBD) remains unclear, it has been suggested that immunologic abnormality has a key role in the pathogenesis of human IBD.[1] Indeed, several immune-regulatory agents, such as corticosteroids, 5-aminosalicylates, immunosuppressants, and anti–tumor necrosis factor (TNF)-α monoclonal antibody, have mainly been used for the treatment of human IBD to control the dysregulated immune response. There are some patients with IBD, however, who are refractory even to the combined use of these agents. In the pathogenesis of IBD, recent clinical and experimental studies have shown that impaired intestinal barrier function permits penetration of toxic and immunogenic factors, which lead to the induction and perpetuation of intestinal inflammation.[2] Therefore, enhancement of intestinal barrier function, which could reduce inflammation caused by decreased uptake of luminal antigens and bacteria, may also provide an effective approach as a novel therapeutic strategy for IBD.

Growth factors have various biologic actions, such as enhancement of cell proliferation, modulation of cell differentiation, and acceleration of cell migration, angiogenesis, and extracellular matrix remodeling.[3,4] A number of growth factors are expressed in the gastrointestinal tract, including members of the epidermal growth factor (EGF) family, the transforming growth factor (TGF)-β family, the fibroblast growth factor (FGF) family, the insulin-like growth factor family, and so on.[5] These growth factors have essential roles in regulating diverse epithelial cell functions, not only to preserve normal homeostasis and the integrity of the intestinal mucosa

*Abbreviations used in this paper:* bFGF, basic fibroblast growth factor; COX, cyclooxygenase; DSS, dextran sulfate sodium; EGF, epidermal growth factor; FGF, fibroblast growth factor; hrbFGF, human recombinant basic fibroblast growth factor; IL, interleukin; ITF, intestinal trefoil factor; KGF, keratinocyte growth factor; MLN, mesenteric lymph nodes; MUC2, mucin 2; PCR, polymerase chain reaction; PPAR, peroxisome proliferator-activated receptor; TGF, transforming growth factor; TNBS, trinitrobenzene sulfonic acid; TNF, tumor necrosis factor; VEGF, vascular endothelial growth factor.


0016-5085/05/$30.00
doi:10.1053/j.gastro.2005.01.006

but also to repair mucosal injury.[5] Therefore, they might serve as an alternative therapy for patients with IBD. Indeed, 2 clinical trials using growth factors were recently performed in patients with active ulcerative colitis. A phase 2 study of keratinocyte growth factor (KGF)-2 in patients with active ulcerative colitis showed that intravenous administration of KGF-2 at a dose of 1–50 μg/kg was not effective for inducing remission.[6] However, a placebo-controlled trial of EGF enemas in patients with active left-sided ulcerative colitis or proctitis showed that the remission rate in the EGF-treated group was significantly higher than in the group receiving placebo.[7] Thus, it has not yet been determined whether growth factors are useful for the treatment of human IBD.

Basic fibroblast growth factor (bFGF, also known as FGF-2) was initially regarded as a potent angiogenic factor because it induces endothelial cell proliferation, migration, and smooth muscle cell proliferation.[8,9] Previous studies have shown that administration of bFGF improved myocardial infarction with developing collateral vessels in experimental models of ischemic heart disease.[10,11] Moreover, based on its pleiotropic function, which has important roles in the differentiation and/or function of the skin, the eye, and the nervous system,[12] bFGF has already been administered as a potential therapeutic agent in various experimental models.[13–20] Those experimental studies showed that bFGF stimulated wound repair in various organs. Additionally, FGF-2 knockout mice show reduced reepithelialization and collagen deposition after skin injury.[21] Those data strongly suggested that bFGF plays a pivotal role in the repair process of wound injury. In the gastrointestinal tract, bFGF enhances epithelial cell proliferation and restitution as well as stem cell survival after radiation injury to the intestine.[22,23] These data suggest that bFGF might be a promising agent in the treatment of mucosal injury in human IBD.

Therefore, in the present study, we examined the efficacy of rectal administration of human recombinant bFGF (hrbFGF) on 2 experimental murine colitis models (ie, dextran sulfate sodium [DSS]-induced colitis and trinitrobenzene sulfonic acid [TNBS]-induced colitis) and investigated the molecular mechanisms of actions of hrbFGF on healing intestinal mucosal injury.

## Materials and Methods

### Animals

Female C57BL/6 mice (8–10 weeks old; Japan SLC, Inc, Shizuoka, Japan) and female SJL/J mice (10–11 weeks old; Charles River Japan, Inc, Kanagawa, Japan) were used for the experiments. They were fed with standard laboratory chow and tap water ad libitum. All mice were housed in specific pathogen–free conditions in the animal facility of Kyoto University. The studies were approved by the animal protection committee of our institution.

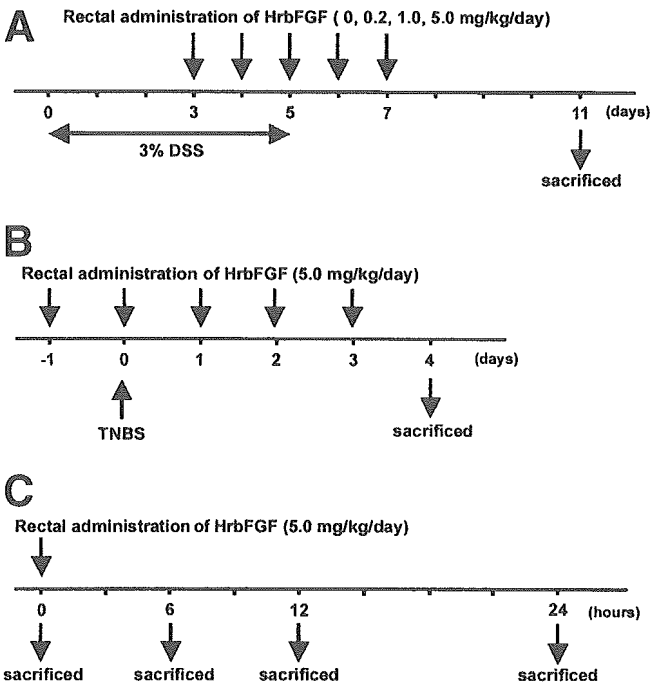


**Figure 1.** Experimental protocols of the study. (*A*) Study with DSS-induced colitis mice; (*B*) study with TNBS-induced colitis mice; and (*C*) study with normal mice.

### Effects of hrbFGF on Experimental Murine Colitis

**DSS-induced colitis model.** *Induction of colitis.* To induce colitis, C57BL/6 mice were given 3% DSS (mol wt, 36–50 kilodaltons; ICN Biomedicals, Inc, Aurora, OH) in their drinking water for 5 days (from day 0 to 4). On day 5, they were switched to regular drinking water. Normal control mice received regular drinking water throughout the experiment.

*Treatments.* Forty mice with DSS-induced colitis were divided into 4 groups (n = 10 in each group) and treated with rectal administration of hrbFGF as follows: 0 (no medication), 0.2, 1.0, or 5.0 mg · $kg^{-1}$ · $day^{-1}$. Another 10 mice were used as normal controls without DSS treatment. hrbFGF was a generous gift from Kaken Pharmaceutical Co Ltd (Tokyo, Japan). hrbFGF was diluted in 150 μL phosphate-buffered saline (PBS) and rectally administered once a day for 5 consecutive days starting from 3 days after the initiation of DSS treatment (Figure 1*A*). After each rectal administration of hrbFGF, mice were kept in an inverted position for 30 seconds. Both normal and nontreated colitis-induced mice received PBS as a vehicle solution via the rectum. Body weight was measured daily throughout the experiment. All mice were monitored for 6 additional days after DSS treatment and killed on

day 11 by cervical dislocation (Figure 1*A*). The colonic tissue was removed from each mouse and examined as described in the following text.

*Macroscopic appearance.* At necropsy, the length from the ileocecal junction to the anal verge was measured as the colonic length.

*Microscopic assessment of colonic damage.* The distal third of the colon was evaluated because this segment is most severely affected in DSS-induced colitis.[24] The entire colon was removed, opened longitudinally, and washed with PBS. The distal third of the colon was dissected, and then the longitudinal section (1.5 cm from the anal verge) was prepared. The sections were fixed in 3.6% formaldehyde, stained with H&E, and histologically analyzed in a blind manner. Histologic damage was quantified by the histologic scoring system described by Williams et al.[25] In brief, the sections were graded as to inflammation severity, inflammation extent, and crypt damage. The grading index for inflammation severity was as follows: 0, none; 1, mild; 2, moderate; 3, severe. The grading index for inflammation extent was as follows: 0, none; 1, mucosa; 2, mucosa and submucosa; 3, transmural. The grading index for crypt damage was as follows: 0, none; 1, basal one third damaged; 2, basal two thirds damaged; 3, crypts lost but surface epithelium present; 4, crypts and surface epithelium lost. Each of these grades was also scored as to the percent involvement (0, 0%; 1, 1%–25%; 2, 26%–50%; 3, 51%–75%; 4, 76%–100%). Each subscore (inflammation severity score, inflammation extent score, and crypt damage score) was the product of the grade multiplied by the percent involvement. The total colitis score was the sum of the 3 subscores.

*Quantitative analysis of gene expressions of proinflammatory cytokine and mucosal repair-related molecules.* Samples of colonic tissue for messenger RNA (mRNA) isolation were removed from the distal third of the colon. Total RNA was extracted using the guanidium isothiocyanate-phenol-chloroform method. RNA (1 μg) was reverse transcribed with MultiScribe reverse transcriptase (Applied Biosystems, Foster City, CA), and the resulting complementary DNAs (50 ng/reaction mixture) were analyzed for TNF-α, cyclooxygenase (COX)-2, TGF-β, mucin 2 (MUC2), intestinal trefoil factor (ITF), and vascular endothelial growth factor (VEGF) mRNA expression by real-time polymerase chain reaction (PCR) using an ABI Prism 7700 sequence detection system (Applied Biosystems). The reaction mixtures were incubated for 2 minutes at 50°C, denatured for 10 minutes at 95°C, and subjected to 45 amplification cycles consisting of annealing and extension at 60°C for 1 minute followed by denaturation at 95°C for 15 seconds. The primers and probes used for this experiment were obtained from Applied Biosystems. Quantification of mRNA was performed using the $\Delta\Delta C_T$ method.[26,27] Gene expression levels of target molecules were normalized using the housekeeping gene, glyceraldehyde-3-phosphate dehydrogenase, amplified using TaqMan rodent glyceraldehyde-3-phosphate dehydrogenase control reagents (Applied Biosystems).

*Flow cytometry analysis for activated T cells in mesenteric lymph nodes.* To investigate the effect of hrbFGF on T cells in vivo, we analyzed the number of activated T cells in mesenteric lymph nodes (MLN) by flow cytometry analysis. On day 8, mice with DSS-induced colitis with or without hrbFGF treatment (5.0 mg · $kg^{-1}$ · $day^{-1}$) were killed, and the MLN were removed (n = 3 in each group; Figure 1*A*). Isolated MLN were gently teased apart using an aseptic 27-gauge needle, and single cells were suspended in RPMI 1640 medium (Invitrogen Corp, Carlsbad, CA) supplemented with 5% heat-inactivated fetal calf serum, 50 μg/mL gentamicin, and 50 μmol/L 2-mercaptoethanol. Cells ($1 \times 10^6$) were preincubated with normal mouse serum for 30 minutes on ice and then stained with both phycoerythrin-conjugated monoclonal antibody against CD4 (BD PharMingen, San Diego, CA) and fluorescein isothiocyanate–conjugated monoclonal antibody against CD69 (BD PharMingen). Cells were washed with PBS and analyzed using a flow cytometer and System II software (EPICS XL; Beckman Coulter, Inc, Fullerton, CA).

**TNBS-induced colitis model.** *Induction of colitis.* TNBS colitis was induced in SJL/J mice by using a modification of the method described by Neurath et al.[28] In brief, 5.0 mg of the hapten reagent TNBS (Sigma Chemical Co, St. Louis, MO) in 50% ethanol was slowly administered into the lumen of the colon (about 4.0 cm from the anal verge) using the catheter fitted onto a 1-mL syringe under diethyl ether anesthesia. Another 5 mice received 50% ethanol alone as vehicle control using the same technique. The total injection volume was 200 μL in both groups. Mice were then kept in an inverted position for 30 seconds. Mice were killed at 4 days after administration of TNBS (Figure 1*B*).

*Treatments.* Mice with TNBS-induced colitis (n = 12) were treated with rectal administration of hrbFGF (5.0 mg · $kg^{-1}$ · $day^{-1}$) for 5 consecutive days, beginning on the day before the initiation of TNBS administration (ie, day −1) (Figure 1*B*). Another 16 mice with TNBS-induced colitis received PBS via rectum as a nontreated group (Figure 1*B*).

*Evaluations.* For assessment of the efficacy of hrbFGF on TNBS-induced colitis, we evaluated the survival rate and histologic findings of colonic tissues. For histologic examination, 2 distal colonic regions spaced approximately 1 cm apart were collected into 3.6% formaldehyde, processed for paraffin embedding, sectioned, and stained with H&E. The degree of colonic inflammation and cryptal regeneration was graded in a blind manner using a histologic scoring system described by Elson et al with some modifications.[29] Briefly, the sections were graded as to inflammation severity, inflammation extent, and regeneration. The grading index for inflammation severity was as follows: 0, none; 1, mild; 2, moderate; 3, severe. The grading index for inflammation extent was as follows: 0, none; 1, mucosa; 2, mucosa and submucosa; 3, transmural. The grading index for regeneration was as follows: 0, complete cryptal regeneration; 1, broad, multifocal cryptal regeneration; 2, partial cryptal regeneration; 3, focal migration and mitotic figures of colonic epithelium or scattered cryptal regeneration; 4, none. Each subscore of 2 histologic segments was averaged.

**Table 1.** Primer Pairs for Semiquantitative PCR

| Target gene | Primer sequences | Major product size (*base pairs*) |
|---|---|---|
| COX-2 | Forward: 5′-gtctgatgatgtatgccaccatctg-3′<br>Reverse: 5′-gcatctggacgaggtttttc-3′ | 658 |
| TGF-β | Forward: 5′-tggaccgcaacaacgccatctatgagaaaacc-3′<br>Reverse: 5′-tggagctgaagcaatagttggtatccagggct-3′ | 525 |
| MUC2 | Forward: 5′-cgacaccagggctttcgcttaat-3′<br>Reverse: 5′-cacttccaccctcccggcaaac-3′ | 501 |
| ITF | Forward: 5′-tctggctaatgctgttggtgg-3′<br>Reverse: 5′-atcagccttgtgttggctgtg-3′ | 388 |
| VEGF | Forward: 5′-cacgacagaaggagagcagaagtc-3′<br>Reverse: 5′-tcaacggtgacgatgatggc-3′ | 594 |
| IL-10 | Forward: 5′-atgcaggactttaagggttacttgggtt-3′<br>Reverse: 5′-atttcggagagaggtacaaacgaggttt-3′ | 455 |
| PPAR-γ | Forward: 5′-cctctccgtgatggaagacc-3′<br>Reverse: 5′-gcattgtgagacatccccac-3′ | 404 |
| β-actin | Forward: 5′-gtgggccgctctaggcaccaa-3′<br>Reverse: 5′-ctctttgatgtcacgcacgatttc-3′ | 540 |

Inflammation score is the sum of inflammation severity and inflammation extent, and thus a score of 8 indicates most severe colonic inflammation. Maximum score of regeneration is 4, indicating no mucosal regeneration, while minimum score is 0, indicating complete mucosal regeneration.

## Effects of hrbFGF on Normal Colonic Mucosa

**Proliferating effects of hrbFGF on intestinal epithelial cells.** To investigate the proliferation activity of hrbFGF on colonic epithelium in vivo, we performed immunohistochemical staining against the Ki-67 antigen. hrbFGF (5.0 mg/kg) was rectally administered to 8-week-old female C57BL/6 mice (n = 3) 24 hours before necropsy. Control mice (n = 3) received PBS alone via the rectum. Paraffin-embedded sections (4 μm thick) were prepared, deparaffinized, and reacted with 0.3% $H_2O_2$ in methanol for 30 minutes to inhibit endogenous peroxidase activity. The sections were placed in 0.01 mol/L citrate buffer (pH 6.0) and pretreated with microwave heating for antigen retrieval. After blocking with 3% bovine serum albumin in PBS, the sections were incubated with anti-mouse Ki-67 monoclonal antibody (Dako Cytomation, Copenhagen, Denmark) diluted 1:200 in PBS with 1% bovine serum albumin overnight at 4°C. After washing with PBS, the sections were incubated with biotinylated anti-rat immunoglobulin G antibody for 30 minutes and then reacted with a peroxidase-linked avidin-biotin complex (Vector Laboratories, Burlingame, CA) diluted 1:100 in PBS with 1% bovine serum albumin for 30 minutes. Localization of the Ki-67 antigen was visualized by incubation with 3,3′-diaminobenzidine tetrahydrochloride in 0.05% $H_2O_2$ for 1 minute. Hematoxylin was used for nuclear counterstaining. Longitudinally sectioned crypts, for which the entire length was visible, were selected in each sample. The number of Ki-67–positive cells in 500 epithelial cells was counted under a microscope at 200× magnification. The Ki-67 labeling index was defined as the percentage of Ki-67–positive cells among the counted epithelial cells.

**Effects of hrbFGF on the gene expression of mucosal repair-related or anti-inflammatory molecules.** Next, we examined the effects of hrbFGF on the gene expression of various molecules involved in the mucosal repair process, such as COX-2, TGF-β, MUC2, ITF, and VEGF by semiquantitative PCR. In addition, we also investigated whether administration of hrbFGF could up-regulate the gene expression of anti-inflammatory molecules, such as interleukin (IL)-10 and peroxisome proliferator-activated receptor (PPAR)-γ. To exclude the influence of inflammatory conditions on those gene expressions, hrbFGF (5.0 mg/kg) was given rectally as a single administration to normal mice. The colonic tissues were collected at 0, 6, 12, and 24 hours after administration of hrbFGF (n = 3 in each group; Figure 1*C*). Total tissue RNA was prepared using the same method as described previously. RNA was reverse transcribed using 5 μg of total RNA according to the manufacturer's instructions. PCR was performed in a volume of 20 μL containing 1 μL of complementary DNA, 0.5 mmol/L of each primer, and a solution of 1 U of *Taq* DNA polymerase using the GeneAmp PCR System 9600 (Perkin-Elmer Corp, Norwalk, CT). The PCR primer sequences used are shown in Table 1. PCR products were separated on 1% agarose gels containing ethidium bromide. After gel electrophoresis, band densities were measured using an autoanalyzing system (Fotodyne, FOTO/Analyst, and Archiver Eclipse; Advanced American Biotechnology, Fullerton, CA). The COX-2, TGF-β, MUC2, ITF, VEGF, IL-10, and PPAR-γ signals were standardized against the β-actin signal for each sample, and results were expressed as the ratio of each molecule to β-actin.

## Effects of hrbFGF on TGF-β Production in Colon-26 and NIH3T3 Cells in Vitro

The murine colonic epithelial cell line Colon-26 and the murine fibroblast cell line NIH3T3 were used for the experiments. Colon-26 cells were maintained with RPMI medium 1640 (Invitrogen Corp) supplemented with 10% heat-inactivated fetal calf serum and antibiotics (100 U/mL peni-

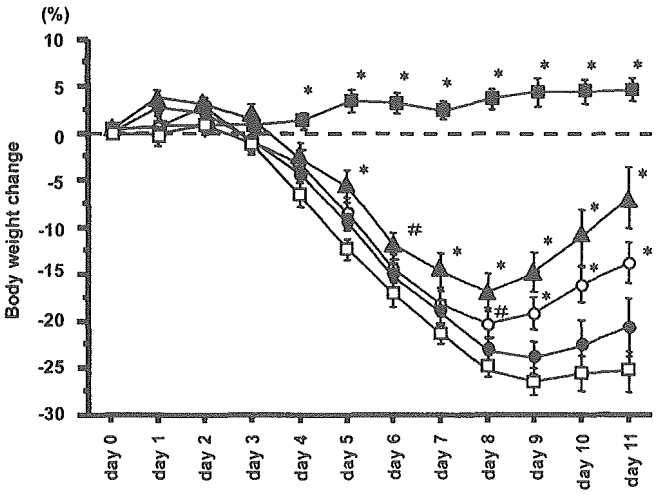


**Figure 2.** Therapeutic effects of hrbFGF on body weight changes in mice with DSS-induced colitis. Serial changes of body weight were measured daily throughout the experiment. Data are expressed as the mean percent change from starting body weight. Results represent means ± SD (n = 10 in each group). *Open squares*, nontreated mice with DSS-induced colitis; *closed circles*, mice with DSS-induced colitis treated with 0.2 mg/kg of hrbFGF; *open circles*, mice with DSS-induced colitis treated with 1.0 mg/kg of hrbFGF; *closed triangles*, mice with DSS-induced colitis treated with 5.0 mg/kg of hrbFGF; *closed squares*, normal mice. $^{*}P < .01$ and $^{\#}P < .05$ compared with nontreated mice with DSS-induced colitis.

cillin and 100 μg/mL streptomycin). NIH3T3 cells were cultured with Dulbecco's modified Eagle medium (ICN Biomedicals, Inc) supplemented with 10% heat-inactivated fetal calf serum and antibiotics (as previously described). Cells were seeded into 24-well plates ($1 \times 10^5$ cells/well) and grown to confluence in basal medium. After that, cells were incubated for 24 hours in serum-free basal medium supplemented with 1% Nutridoma-SP (Roche Diagnostics Corp, Indianapolis, IN) and then were stimulated with hrbFGF (100 ng/mL) plus heparin (10 μg/mL). The conditioned media were collected at the indicated points and assessed for the amount of total TGF-β1 protein by enzyme-linked immunosorbent assay using a TGF-β1 $E_{max}$ ImmunoAssay System (Promega Corp, Madison, WI) according to the manufacturer's instructions.

### Statistical Analysis

Student *t* test and the Mann–Whitney *U* test were used where appropriate for statistical analysis. Cumulative survival rate was calculated by the Kaplan–Meier method, and survival curves were compared by log-rank test. The data are expressed as mean ± SD. A 2-tailed *P* value of $<.05$ was considered statistically significant.

## Results

### Effects of hrbFGF on DSS-Induced Colitis

**Body weight change.** In the nontreated mice with DSS-induced colitis, body weight gradually decreased and did not recover at the end of the experiment. On the other hand, the body weight in mice with DSS-induced colitis treated with 1.0 or 5.0 mg/kg of hrbFGF significantly recovered in a dose-dependent manner compared with the nontreated mice with DSS-induced colitis (Figure 2).

**Colonic length.** The colonic length in the nontreated mice with DSS-induced colitis was significantly shorter than in normal mice. The colonic length in mice with DSS-induced colitis treated with 5.0 mg/kg of hrbFGF was significantly greater than in the nontreated mice with DSS-induced colitis ($P < .01$). However, there were no significant differences in colonic length between the nontreated mice with DSS-induced colitis and the groups treated with 0.2 or 1.0 mg/kg of hrbFGF (Figure 3).

**Representative histologic findings of the colonic tissues.** In both the nontreated and hrbFGF-treated (5.0 mg/kg) mice with DSS-induced colitis, the histologic findings revealed epithelial destruction, remarkable infiltration of inflammatory cells, and submucosal edema (Figure 4*B* and *C*). In contrast, in mice with DSS-induced colitis treated with 1.0 mg/kg of hrbFGF, crypt regeneration and restoration of colonic mucosa were observed, although there was a limited amount of cellular infiltration and edema in the lamina propria and submucosa (Figure 4*D*). Moreover, histologic findings of mice with DSS-induced colitis treated with 5.0 mg/kg of hrbFGF were essentially normal (except in 3 mice), al-

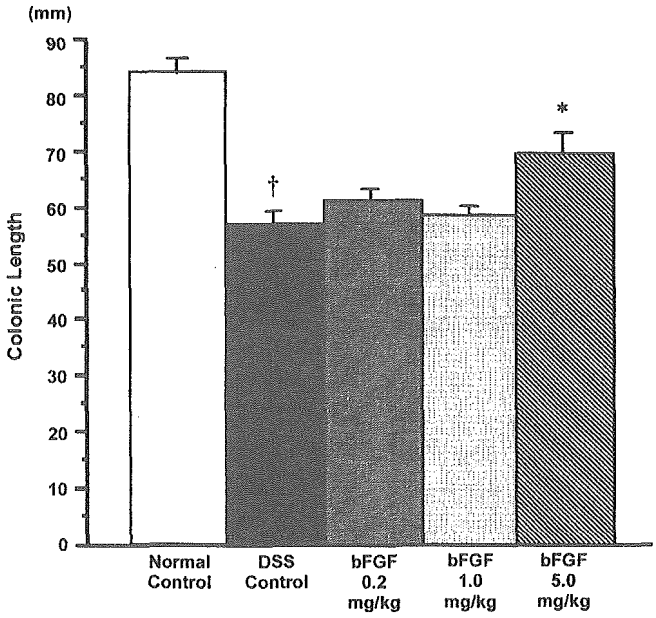


**Figure 3.** Effects of rectal administration of hrbFGF on colonic length in mice with DSS-induced colitis. Colonic length was measured from the ileocecal junction to the anal verge at necropsy (on day 11). Data are expressed as means ± SD (n = 10 in each group). $^{*}P < .01$ compared with nontreated mice with DSS-induced colitis. $^{\dagger}P < .01$ compared with normal mice.

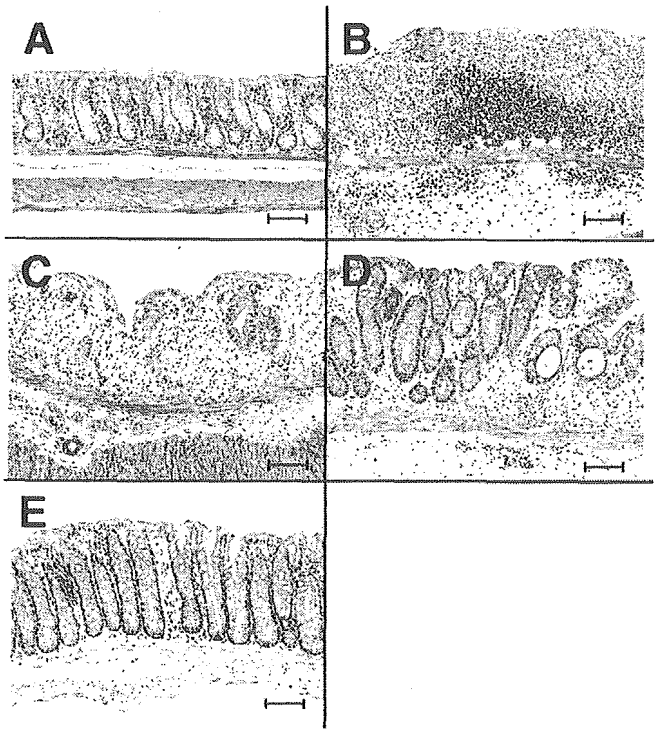


**Figure 4.** Representative histologic findings in mice with DSS-induced colitis treated with hrbFGF. Sections of the distal colon were collected at necropsy (on day 11) and stained with H&E. (*A*) Normal mice, (*B*) nontreated mice with DSS-induced colitis, (*C*) mice with DSS-induced colitis treated with 0.2 mg/kg of hrbFGF, (*D*) mice with DSS-induced colitis treated with 1.0 mg/kg of hrbFGF, and (*E*) mice with DSS-induced colitis treated with 5.0 mg/kg of hrbFGF. *Bars* = 100 μm. (Original magnification 200×.)

though there was slight infiltration of mononuclear cells and neutrophils (Figure 4*E*).

**Histologic evaluation.** Rectal administration of 1.0 or 5.0 mg/kg of hrbFGF dose-dependently and significantly reduced both the subscores and the total colitis scores in mice with DSS-induced colitis compared with the nontreated mice with DSS-induced colitis (Figure 5). On the other hand, administration of 0.2 mg/kg of hrbFGF significantly improved only the inflammatory severity score (Figure 5).

**Gene expression of proinflammatory cytokines and mucosal repair-related molecules in mice with DSS-induced colitis with and without hrbFGF treatment.** The gene expression of TNF-α and COX-2 in the nontreated mice with DSS-induced colitis was significantly higher than in normal mice. mRNA expression of TNF-α and COX-2 in mice with DSS-induced colitis treated with 5.0 mg/kg of hrbFGF was significantly lower than in the nontreated mice with DSS-induced colitis (Figure 6). There were no significant differences in TNF-α and COX-2 expression between the nontreated and hrbFGF-treated (0.2 or 1.0 mg/kg) mice with DSS-induced colitis (Figure 6). Similar trends were observed in TGF-β and VEGF mRNA expression in mice with DSS-induced colitis treated with hrbFGF, although there was no statistical significance (Figure 6). On the other hand, gene expression of MUC2 and ITF in the nontreated mice with DSS-induced colitis was significantly lower than in normal mice. However, treatment with 5.0 mg/kg of hrbFGF significantly increased both MUC2 and ITF mRNA expression as compared with the nontreated mice with DSS-induced colitis and was even higher than in normal mice, although there were no significant differences (Figure 6).

**Expression of CD69 on $CD4^+$ T cells from MLN.** There were no significant differences in the number of $CD4^+$ T cells from the MLN between mice with DSS-induced colitis treated with and without hrbFGF ($5.22 \pm 0.59 \times 10^6$ vs $4.81 \pm 0.49 \times 10^6$; $P = .248$). In addition, similar results were observed in the number of $CD4^+CD69^+$ T cells from MLN ($10.65 \pm 0.58 \times 10^5$ vs $9.78 \pm 0.11 \times 10^5$; $P = .564$).

## Effects of hrbFGF on TNBS-Induced Colitis

**Cumulative survival rate.** The overall survival rate of mice with TNBS-induced colitis treated with hrbFGF (5.0 mg/kg) was significantly higher than that of the nontreated mice with TNBS-induced colitis (91.7% vs 56.3%; $P = .0421$; Figure 7*A*).

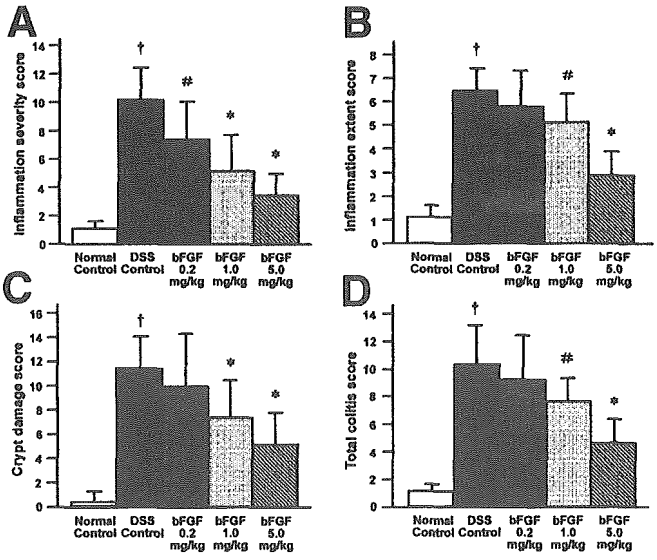


**Figure 5.** Histologic scores of colonic tissues in mice with DSS-induced colitis treated with hrbFGF. Each subscore was the product of the grade multiplied by the percent involvement. The total colitis score is the sum of the 3 subscores (inflammation severity, inflammation extent, and crypt damage). (*A*) Inflammation severity score, (*B*) inflammatory extent score, (*C*) crypt damage score, and (*D*) total colitis score. Data are expressed as means ± SD (n = 10 in each group). $^*P < .01$ and $^\#P < .05$ compared with nontreated mice with DSS-induced colitis. $^\dagger P < .01$ compared with normal mice.

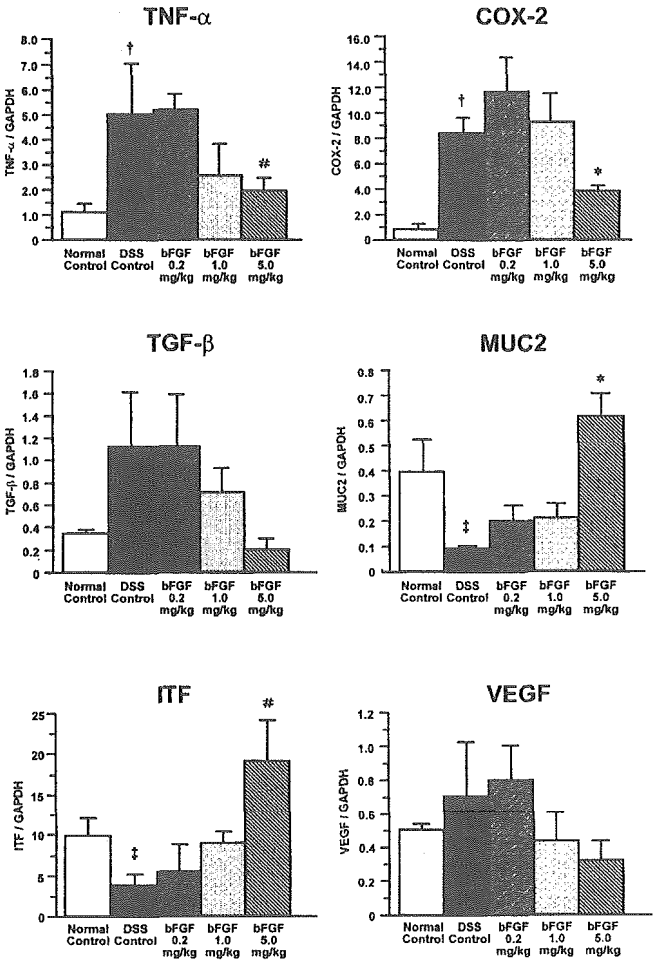


**Figure 6.** Effects of rectal administration of hrbFGF on the transcript levels of TNF-α, COX-2, TGF-β, MUC2, ITF, and VEGF in the colonic tissues of mice with DSS-induced colitis. The gene expression of each target molecule was determined by real-time PCR and was standardized against glyceraldehyde-3-phosphate dehydrogenase. Data are expressed as means ± SD (n = 5 in each group). $^{*}P < .01$ and $^{\#}P < .05$ compared with nontreated mice with DSS-induced colitis. $^{\dagger}P < .01$ and $^{\ddagger}P < .05$ compared with normal mice.

**Representative histologic findings of the colonic tissues.** In the nontreated mice with TNBS-induced colitis, the histologic analysis showed lymphocytic infiltrates, ulcerations, loss of cryptal cells, and thickening of the colonic wall. In contrast, in mice with TNBS-induced colitis treated with hrbFGF (5.0 mg/kg), reepithelialization and cryptal regeneration of colonic mucosa were partially observed, although lymphocytic infiltrates still remained (Figure 7*B*).

**Histologic evaluation.** Rectal administration of hrbFGF (5.0 mg/kg) did not significantly reduce inflammation score in the hrbFGF-treated group compared with the nontreated group (Figure 7*C*). On the contrary, regeneration score in the group treated with hrbFGF tended to be lower than in the nontreated group, although there was no significant difference (Figure 7*C*).

## Effects of hrbFGF on Normal Colonic Mucosa

**Immunohistochemical staining with anti-Ki-67 monoclonal antibody.** In control mice, Ki-67–positive cells were mainly located in the lower third of the crypts (Figure 8*A*, left panel). On the other hand, in mice treated with hrbFGF, Ki-67–positive cells were observed in the lower to middle third of the crypts (Figure 8*A*, right panel). The Ki-67 labeling index in mice treated with hrbFGF was significantly higher than in control mice (Figure 8*B*).

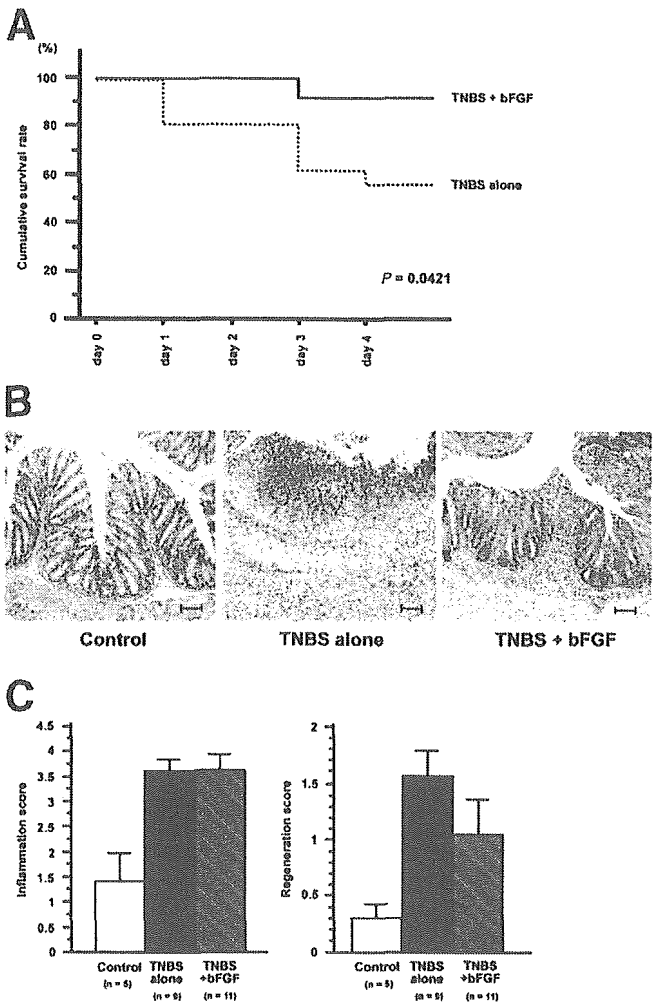


**Figure 7.** Effects of rectal administration of hrbFGF on murine TNBS-induced colitis. (*A*) Cumulative survival curves in mice with TNBS-induced colitis. *Solid line*, mice with TNBS-induced colitis treated with 5.0 mg/kg of hrbFGF; *dotted line*, nontreated mice with TNBS-induced colitis. (*B*) Representative histologic findings in mice with TNBS-induced colitis. Control, control mice receiving 50% ethanol alone; TNBS alone, nontreated mice with TNBS-induced colitis; TNBS + bFGF, mice with TNBS-induced colitis treated with 5.0 mg/kg of hrbFGF. *Bars* = 100 μm. (Original magnification 100×.) (*C*) Histologic scores (inflammation score and regeneration score) of colonic tissues in mice with TNBS-induced colitis treated with hrbFGF. Inflammation score is the sum of inflammatory severity and inflammatory extent. Data are expressed as means ± SD.